Table of contents

Figure S1: ESI-TOF LC-MS of Qβ-glycan conjugate **1**with peaks from Qβ coat protein monomer and the respective Qβ–glycan conjugates marked. Assuming Qβ monomer and Qβ-glycan conjugates have the same ionizing efficiencies, the ion intensities of the peaks were used to estimate the relative quantities of each species. On average, there were 1.61 glycan **1** per Qβ monomer, which corresponds to 290 copies of glycan **1** per Qβ particle.

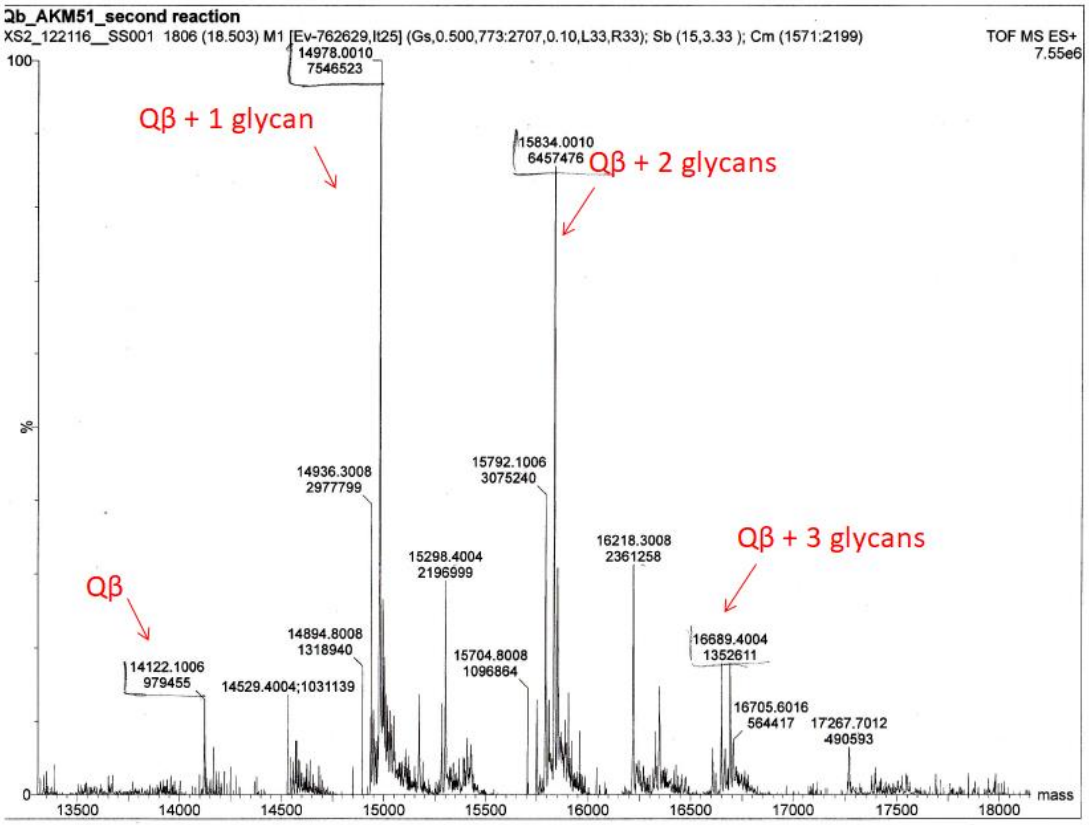

Figure S2: MALDI-TOF MS of BSA-glycan **1** conjugate**.** Based on the molecular weight difference between the BSA-glycan **1** conjugate and unmodified BSA, the number of glycan **1** per BSA was calculated to be 15.

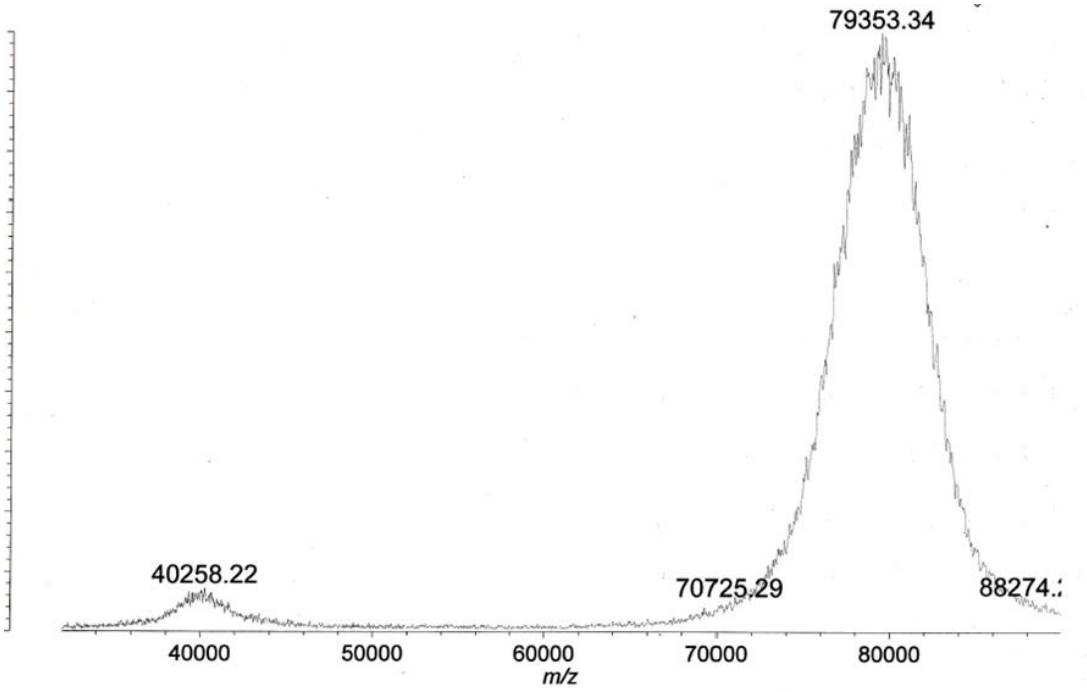

Figure S3. The titers of anti-glycan antibody subtypes elicited by Qβ-glycan **1**from mice (day 35, 4 μg). ELISA titers were calculated as the highest fold of serum dilution that gave optical density of 0.1 higher than the background in ELISA assays. Each symbol represents one mouse, with the long horizontal line for each group representing the mean value of each group.

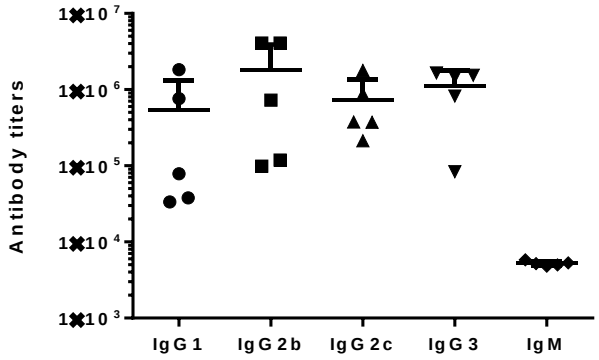

Table S1. a) Anti-glycan **1**IgG ELISA titers from rabbits immunized with Qβ-glycan **1** conjugate. b) Anti-*S.* Paratyphi A OPS IgG ELISA titers from rabbits immunized with Qβ-glycan **1** conjugate.

a)

	anti-glycan 1 IgG (ELISA unit)			
	Pre-immunization	**Day 35 post immunization**	**Day 49 post immunization**	**Day 56 post immunization**
Rabbit 1	<2,000	1.2×10^7	1.4×10^7	1.4×10^7
Rabbit 2	<2,000	1.6×10^7	2.1×10^7	1.2×10^7

b)

	anti-Paratyphi A OPS IgG (ELISA unit)	
	Pre-immunization	**Day 56 post immunization**
Rabbit 1	181	1.8×10^6
Rabbit 2	84	2.4×10^6

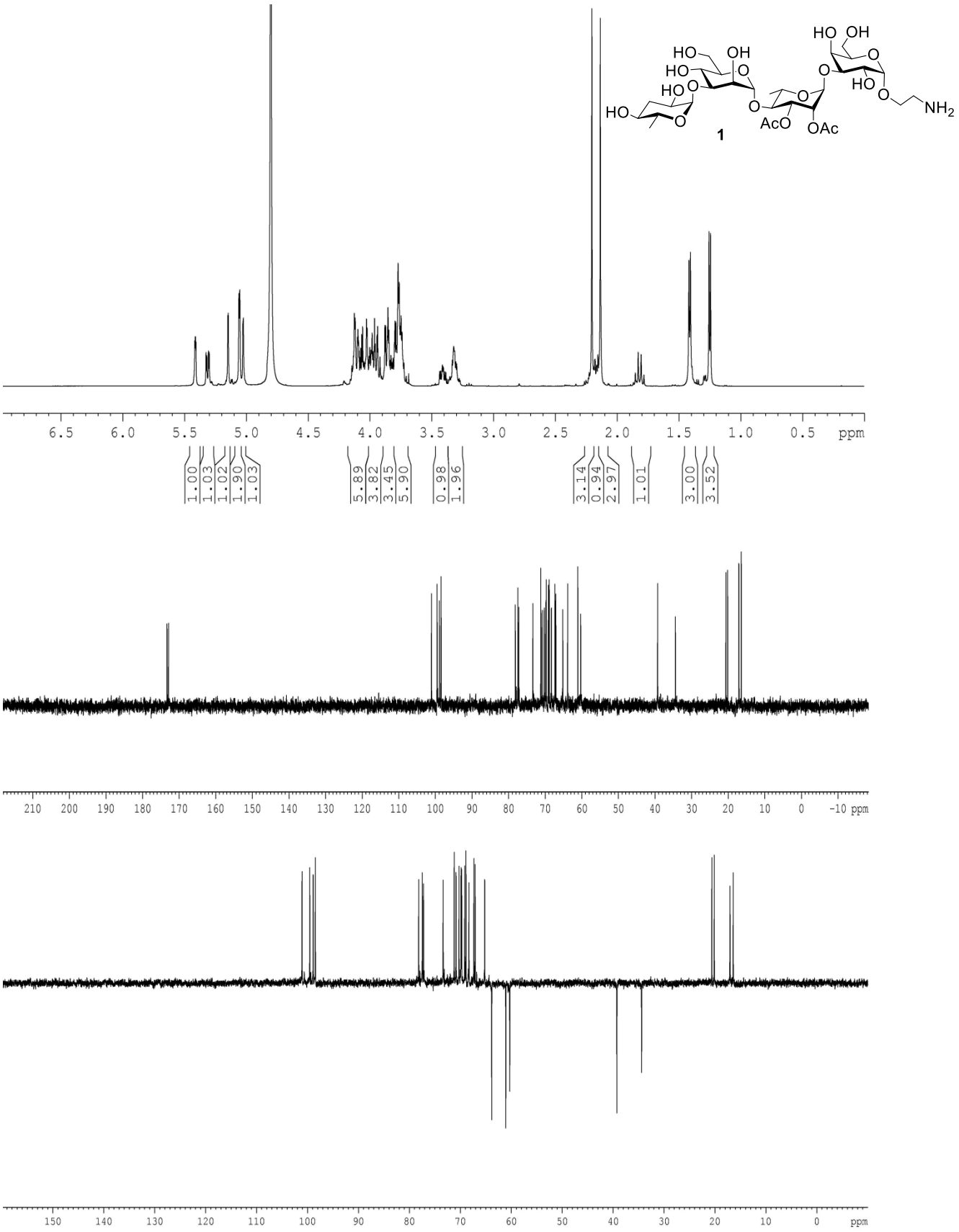

^{1}H, ^{13}C and DEPT-135 NMR spectra of 2-aminoethyl (3,6-dideoxy-α-D-*ribo*-hexopyranosyl)-(1→3)-(α-D-mannopyranosyl)-(1→4)-(2,3-di-*O*-acetyl-α-L-rhamnopyranosyl)-(1→3)-α-D-galactopyranoside (**1**) (D_2O, 500 MHz).

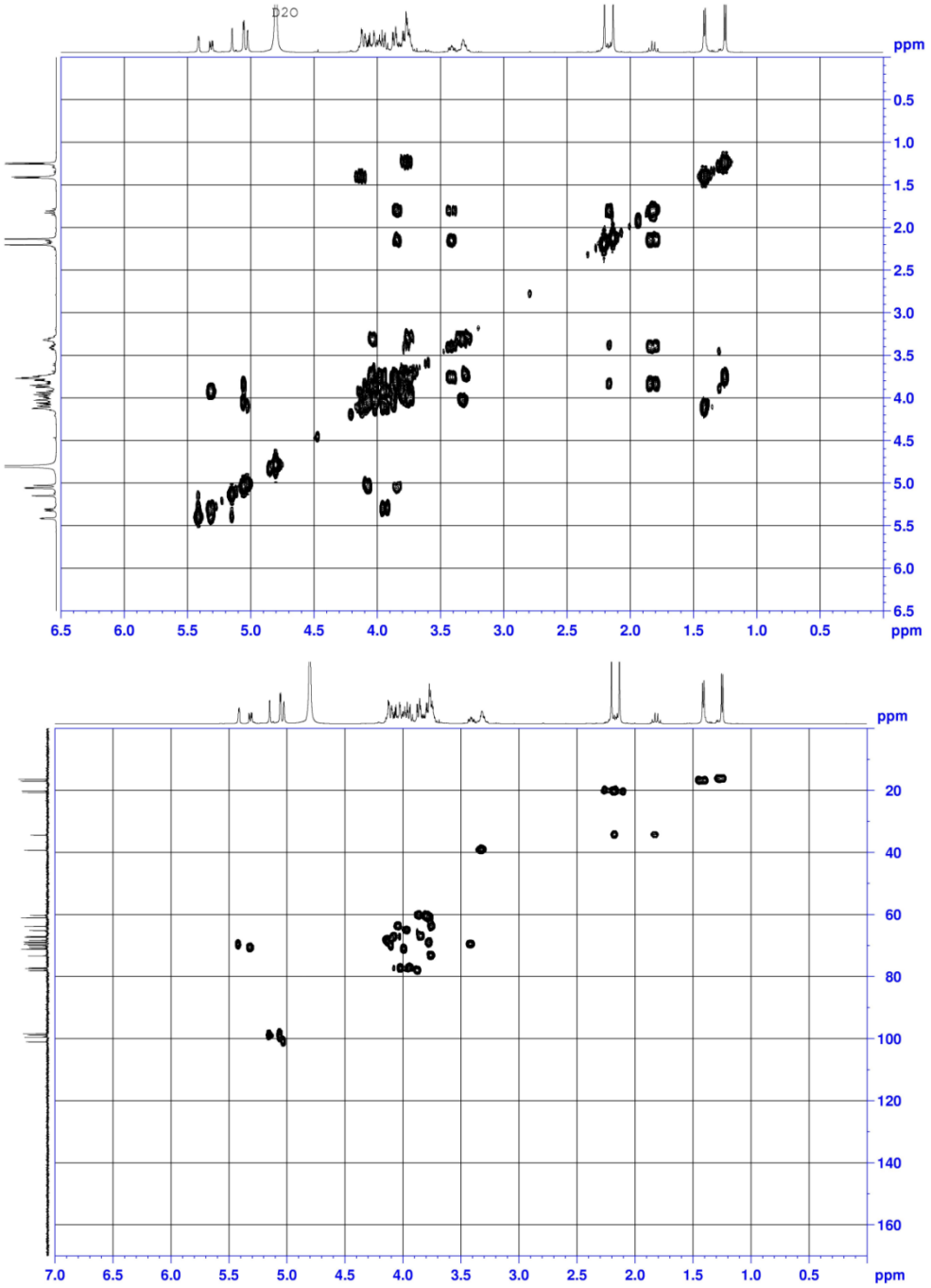

2D COSY and HSQC NMR spectra of 2-aminoethyl (3,6-dideoxy-α-D-*ribo*-hexopyranosyl)-(1→3)-(2,3-di-*O*-acetyl-α-D-mannopyranosyl)-(1→4)-(α-L-rhamnopyranosyl)-(1→3)-α-D-galactopyranoside (**1**) (D_2O, 500 MHz).

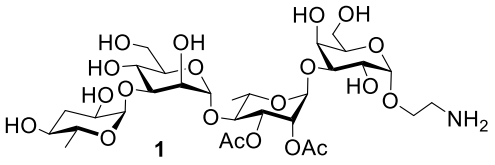

1

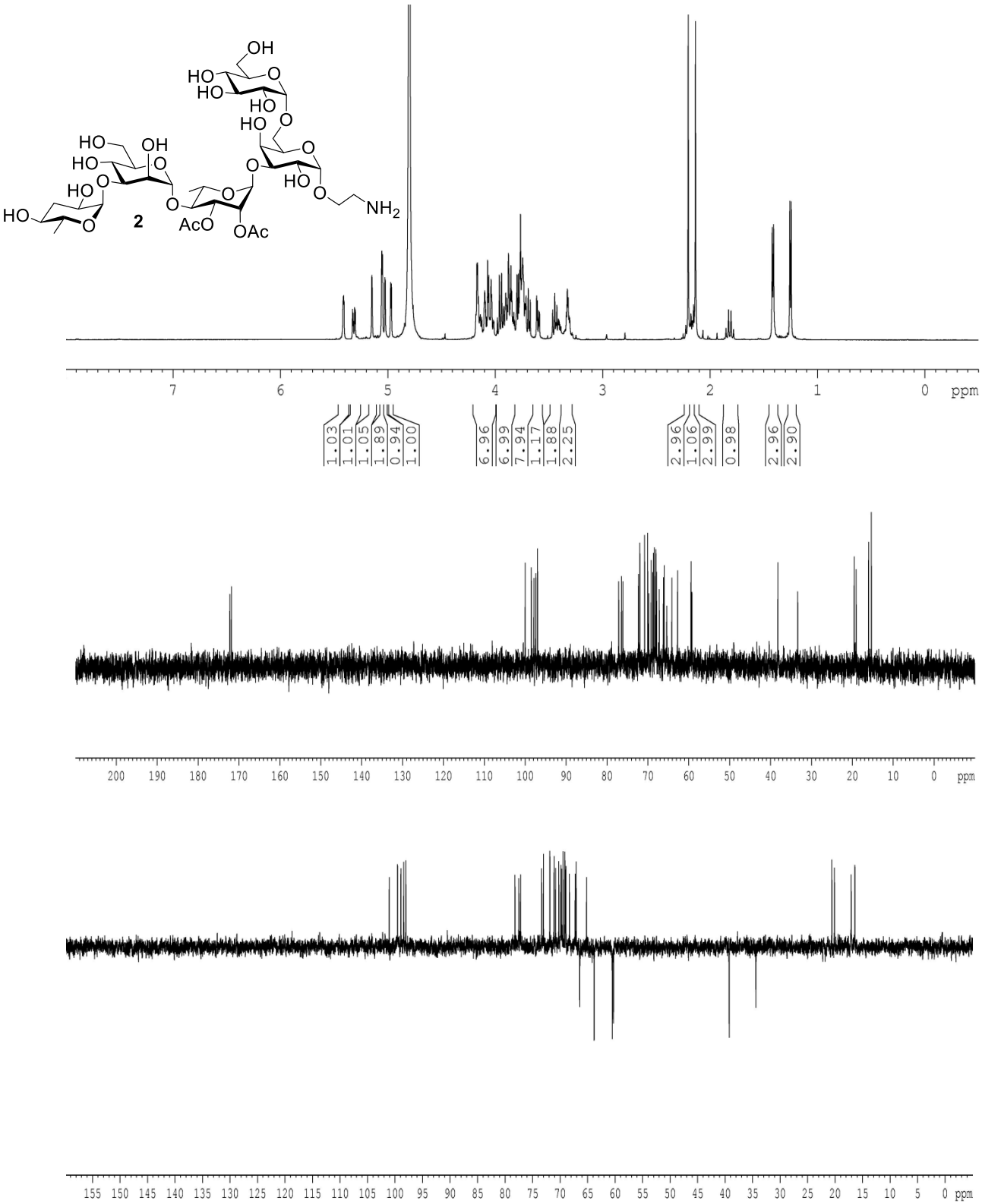

^{1}H, ^{13}C and DEPT-135 NMR spectra of 2-azidoethyl (3,6-dideoxy-α-D-*ribo*-hexopyranosyl)-(1→3)-(α-D-mannopyranosyl)-(1→4)-(2,3-di-*O*-acetyl-α-L-rhamnopyranosyl)-(1→3)-[(α-D-glucopyranosyl)-(1→6)]-α-D-galactopyranoside (**2**) (D_2O, 500 MHz).

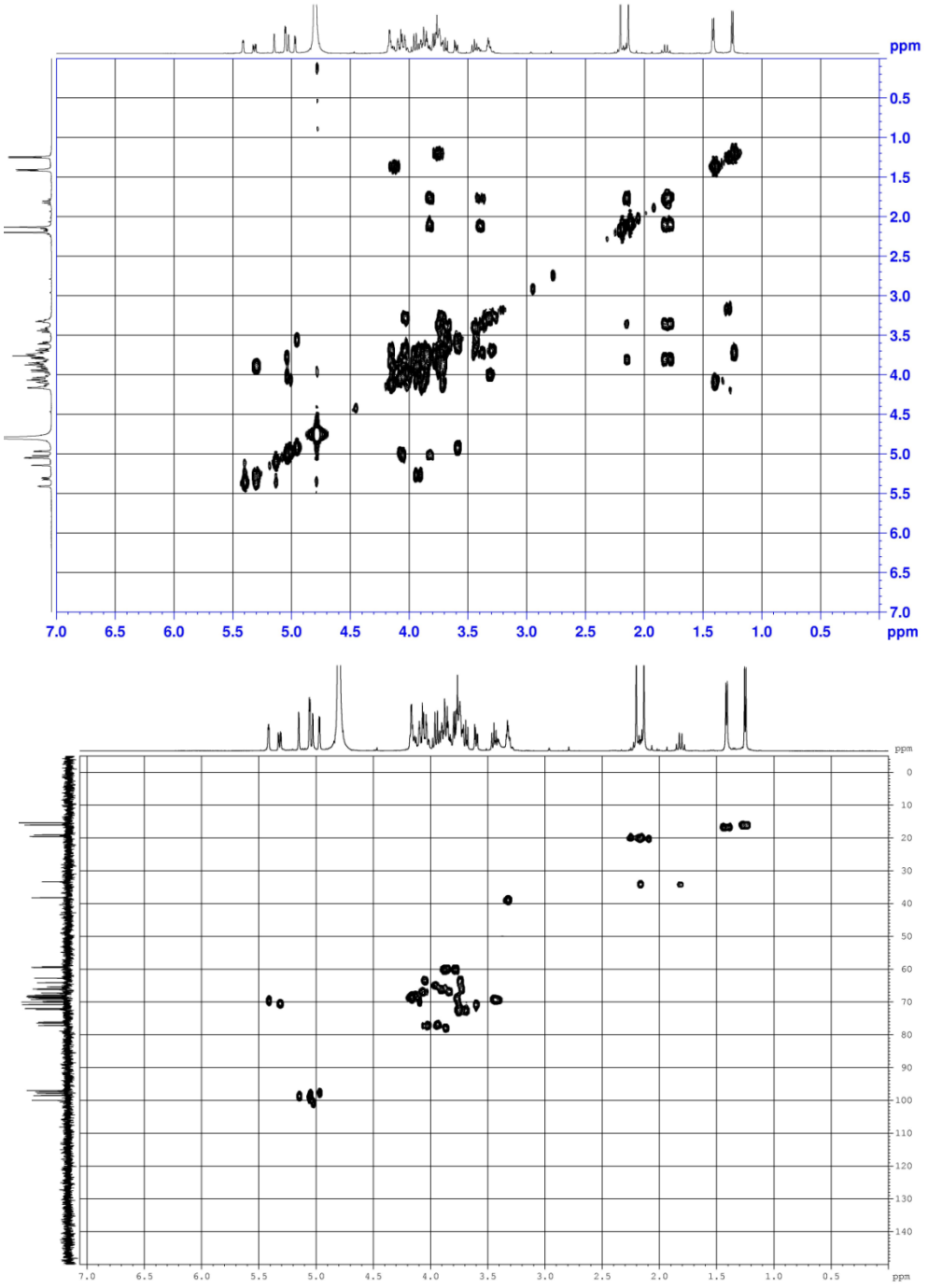

2D COSY and HSQC NMR spectraof 2-azidoethyl (3,6-dideoxy-α-D-*ribo*-hexopyranosyl)-(1→3)-(α-D-mannopyranosyl)-(1→4)-(2,3-di-*O*-acetyl-α-L-rhamnopyranosyl)-(1→3)-[(α-D-glucopyranosyl)-(1→6)]-α-D-galactopyranoside (**2**) (D_2O, 500 MHz).

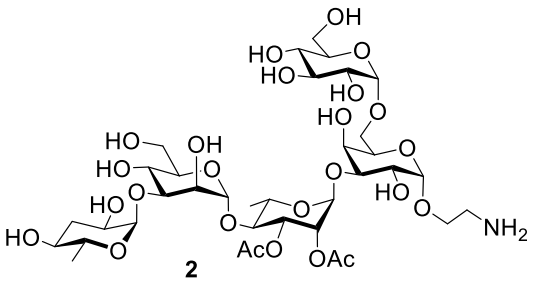

2

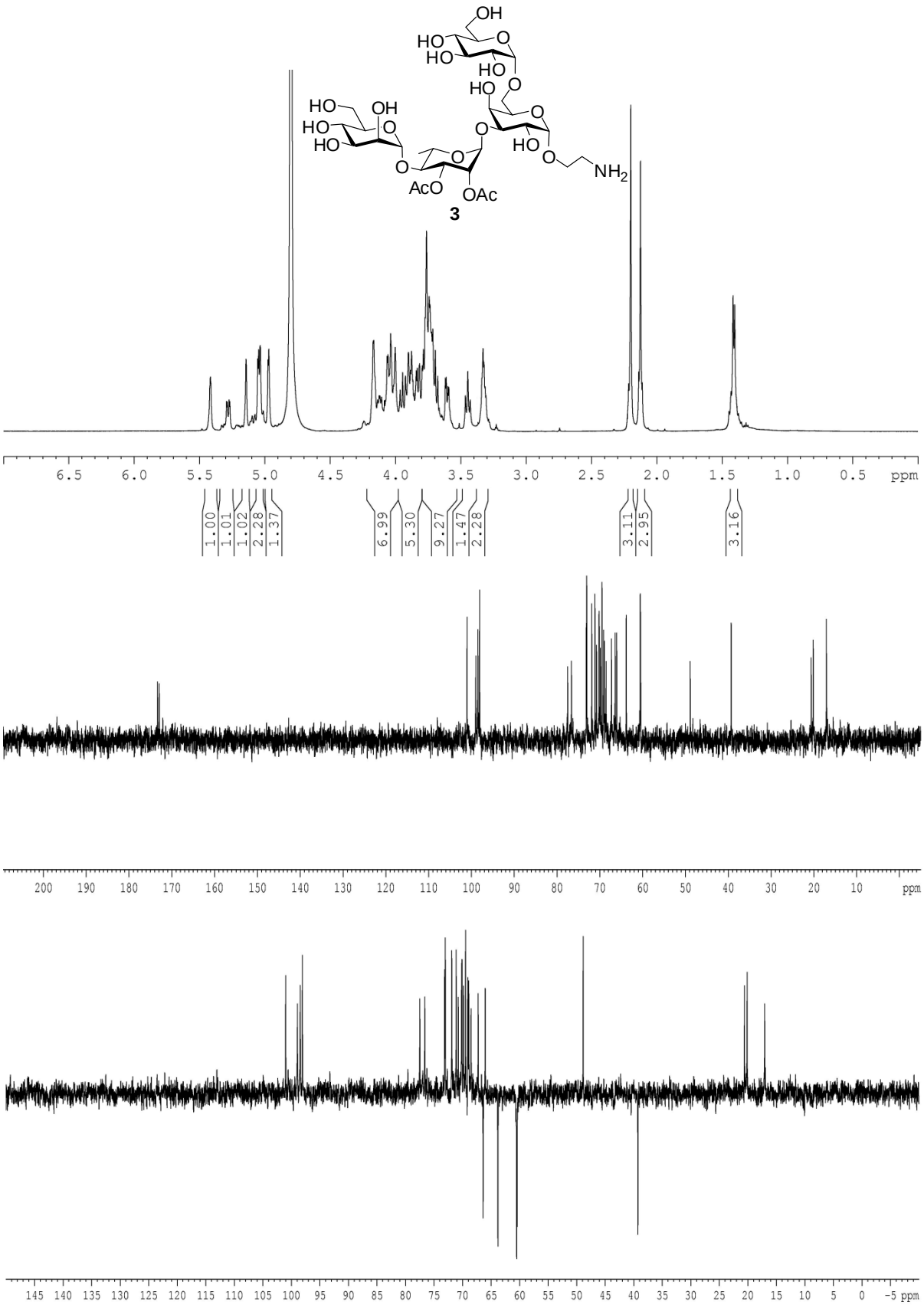

^{1}H, ^{13}C and DEPT-135 NMR spectra of 2-azidoethyl (α-D-mannopyranosyl)-(1→4)-(2,3-di-*O*-acetyl-α-L-rhamnopyranosyl)-(1→3)-[(α-D-glucopyranosyl)-(1→6)]-α-D-galactopyranoside (**3**)(D_2O, 500 MHz).

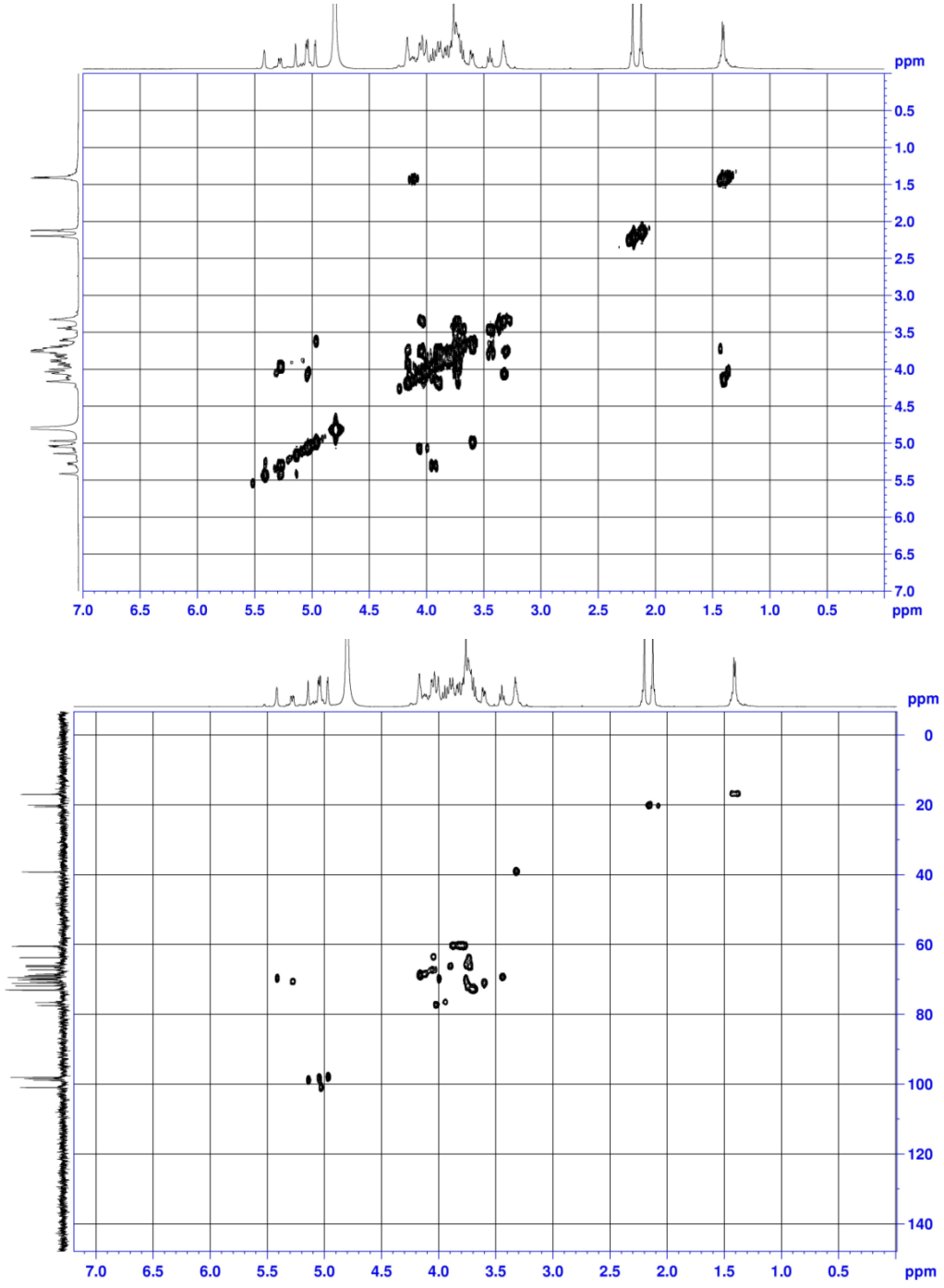

2D COSY and HSQC NMR spectra of 2-azidoethyl (α-D-mannopyranosyl)-(1→4)-(2,3-di-*O*-acetyl-α-L-rhamnopyranosyl)-(1→3)-[(α-D-glucopyranosyl)-(1→6)]-α-D-galactopyranoside (**3**)(D_2O, 500 MHz).

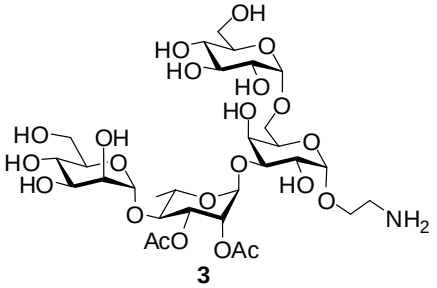

3

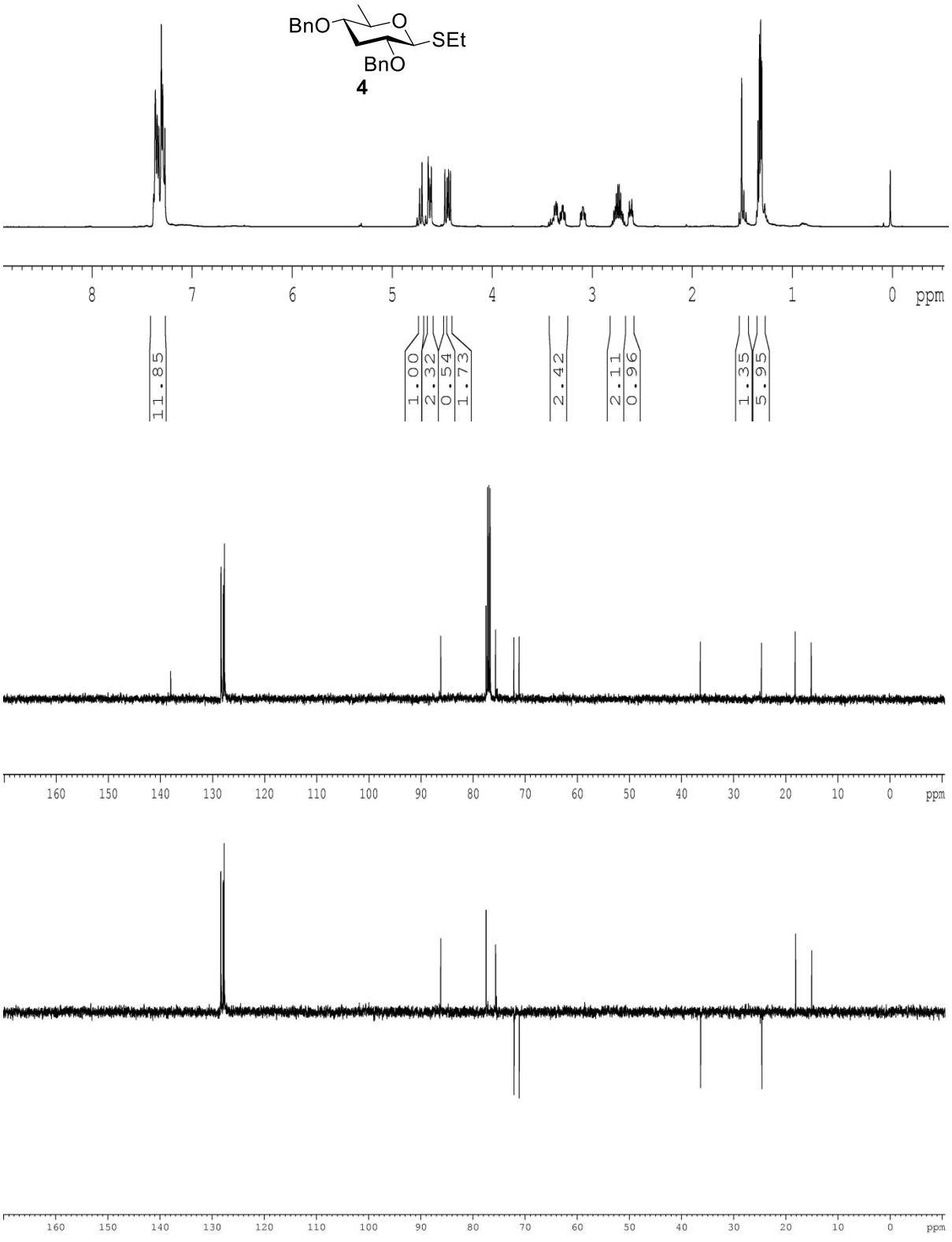

^{1}H, ^{13}C and DEPT-135 NMR spectra of ethyl 2,4-di-*O*-benzyl-3,6-dideoxy-1-thio-β-D-ribohexopyranoside (**4**) ($CDCl_3$, 500 MHz).

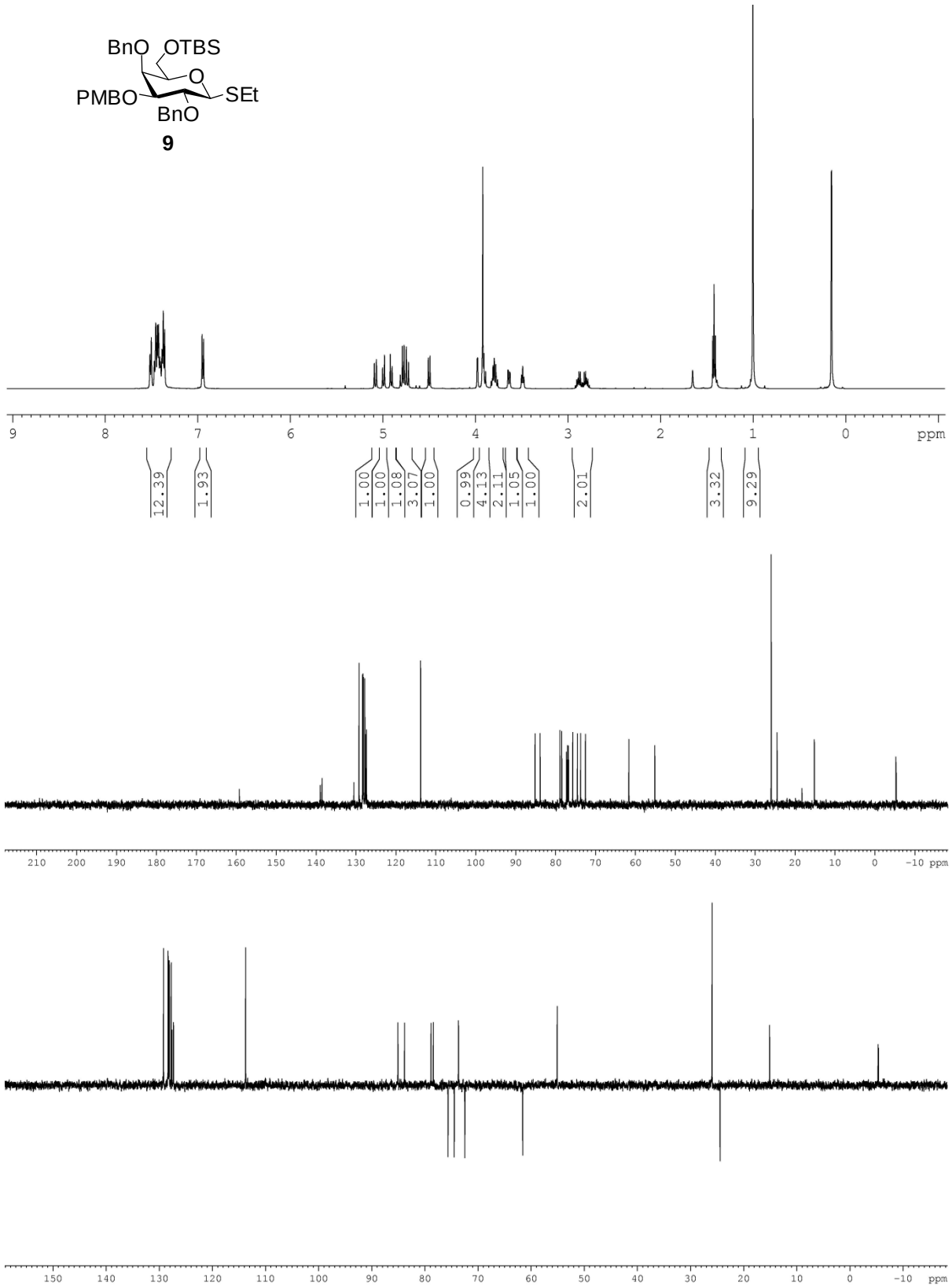

^{1}H, ^{13}C and DEPT-135 NMR spectra of ethyl 2,4-di-*O*-benzyl-3-*O*-*p*-methoxybenzyl-6-*O*-(tert-butyldimethylsilyl)-1-thio-β-D-galactopyranoside(**9**) ($CDCl_3$, 500 MHz).

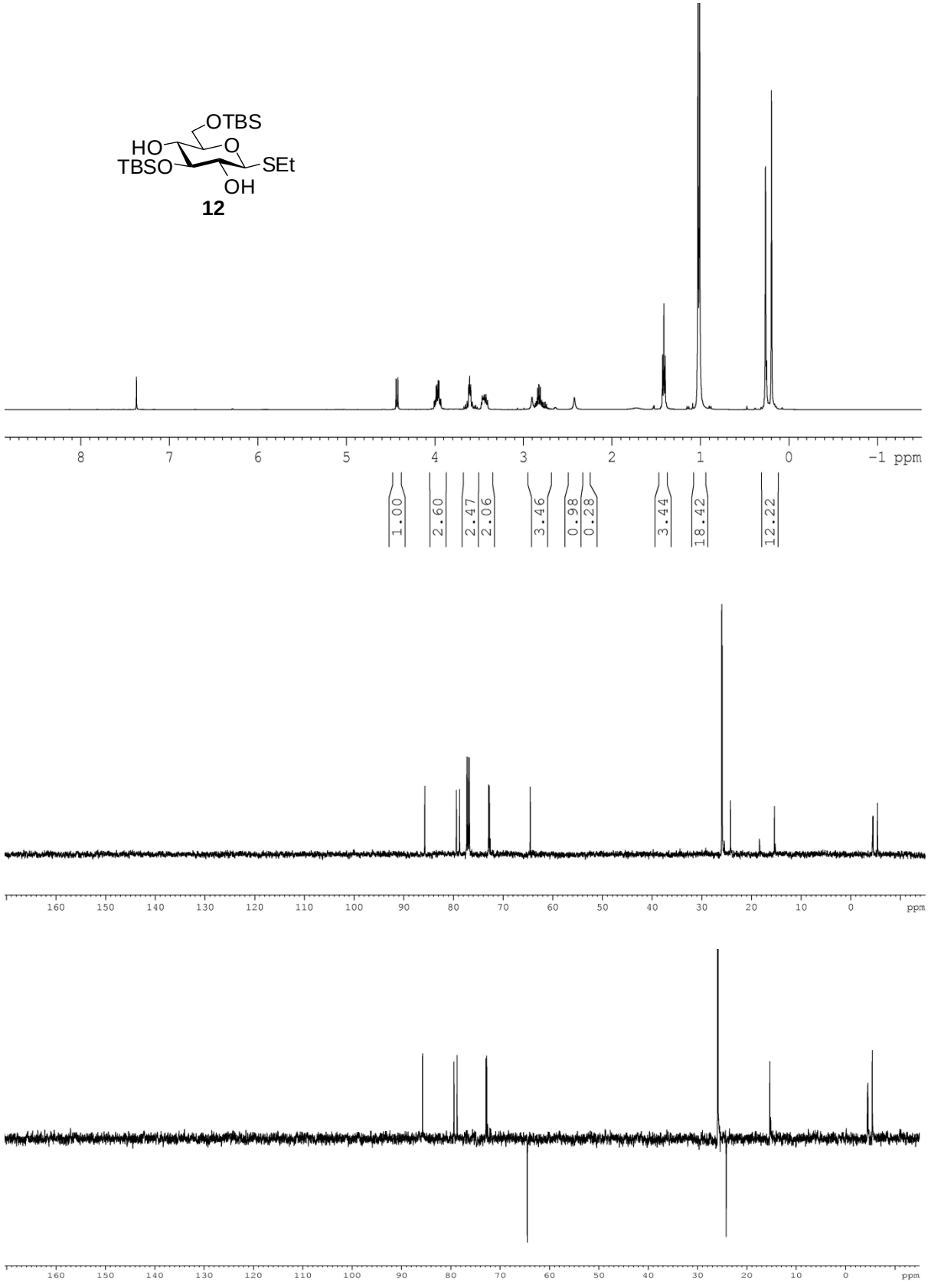

^{1}H, ^{13}C and DEPT-135 NMR spectra of ethyl 3,6-di-*O*-(tert-butyldimethylsilyl)-1-thio-β-D-glucopyranoside (**12**)($CDCl_3$, 500 MHz).

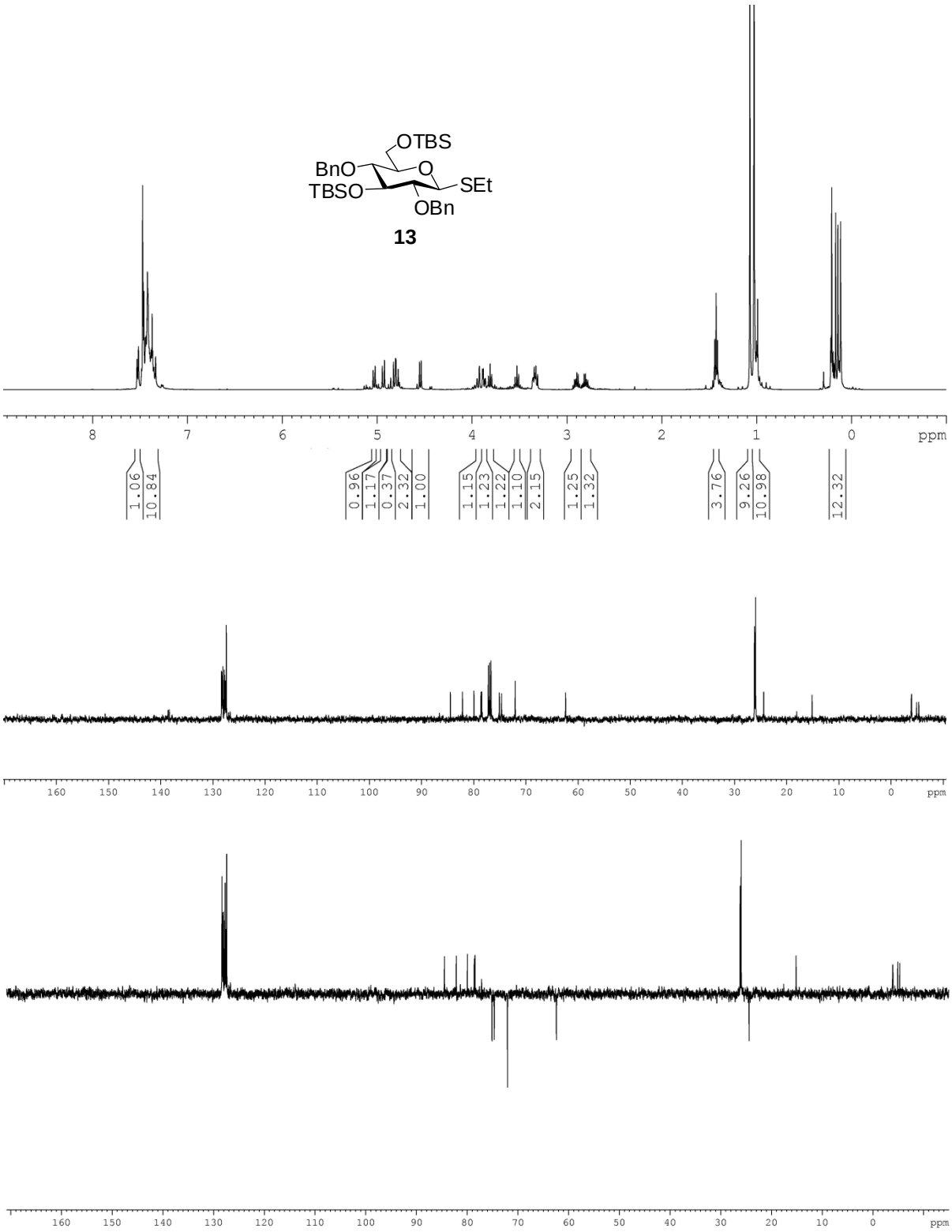

^{1}H, ^{13}C and DEPT-135 NMR spectra of ethyl 2,4-di-*O*-benzyl-3,6-di-*O*-(tert-butyldimethylsilyl)-1-thio-β-D-glucopyranoside (**13**) ($CDCl_3$, 500 MHz).

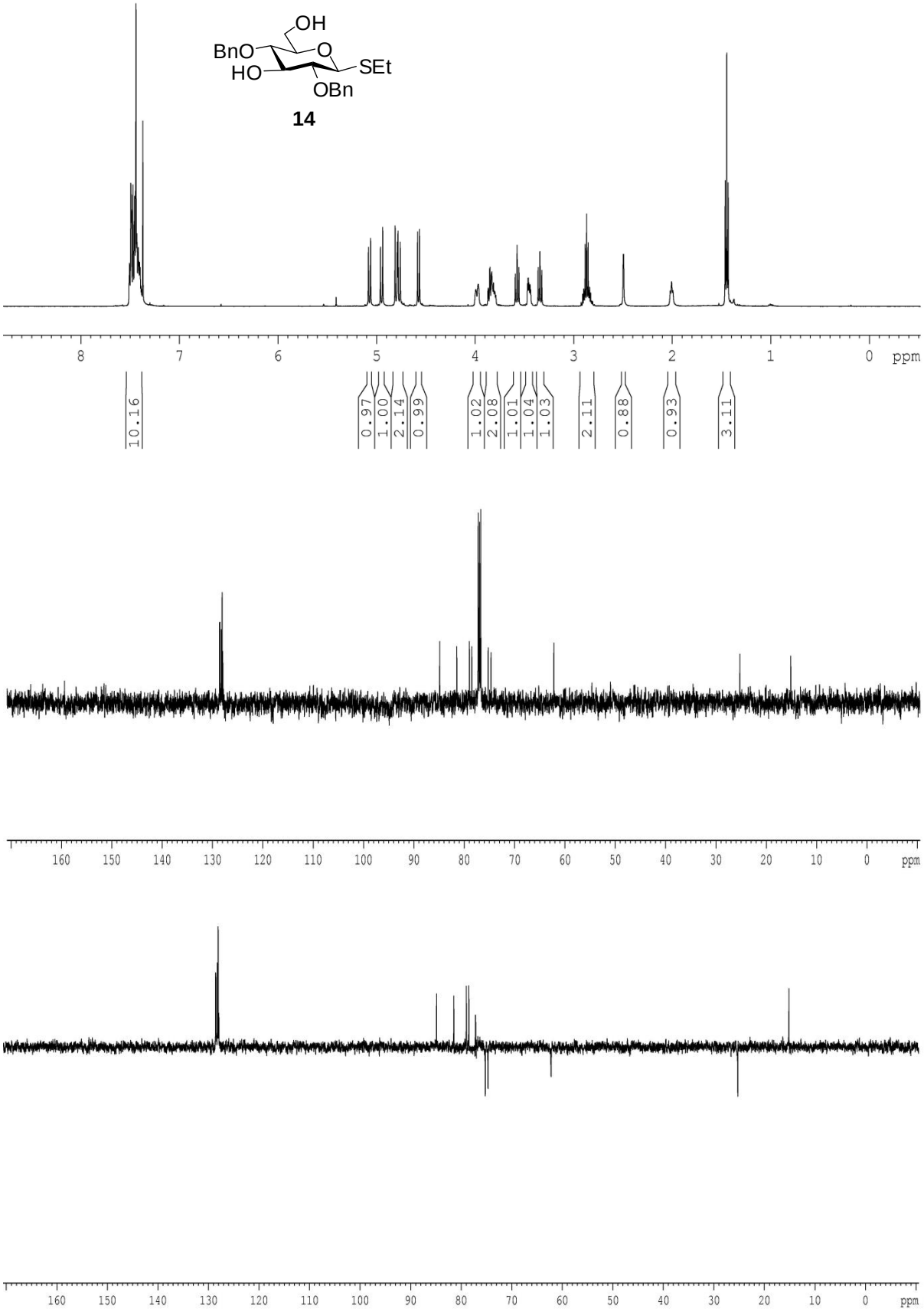

^{1}H, ^{13}C and DEPT-135 NMR spectra of ethyl 2,4-di-*O*-benzyl-1-thio-α-D-glucopyranoside (**14**) ($CDCl_3$, 500 MHz).

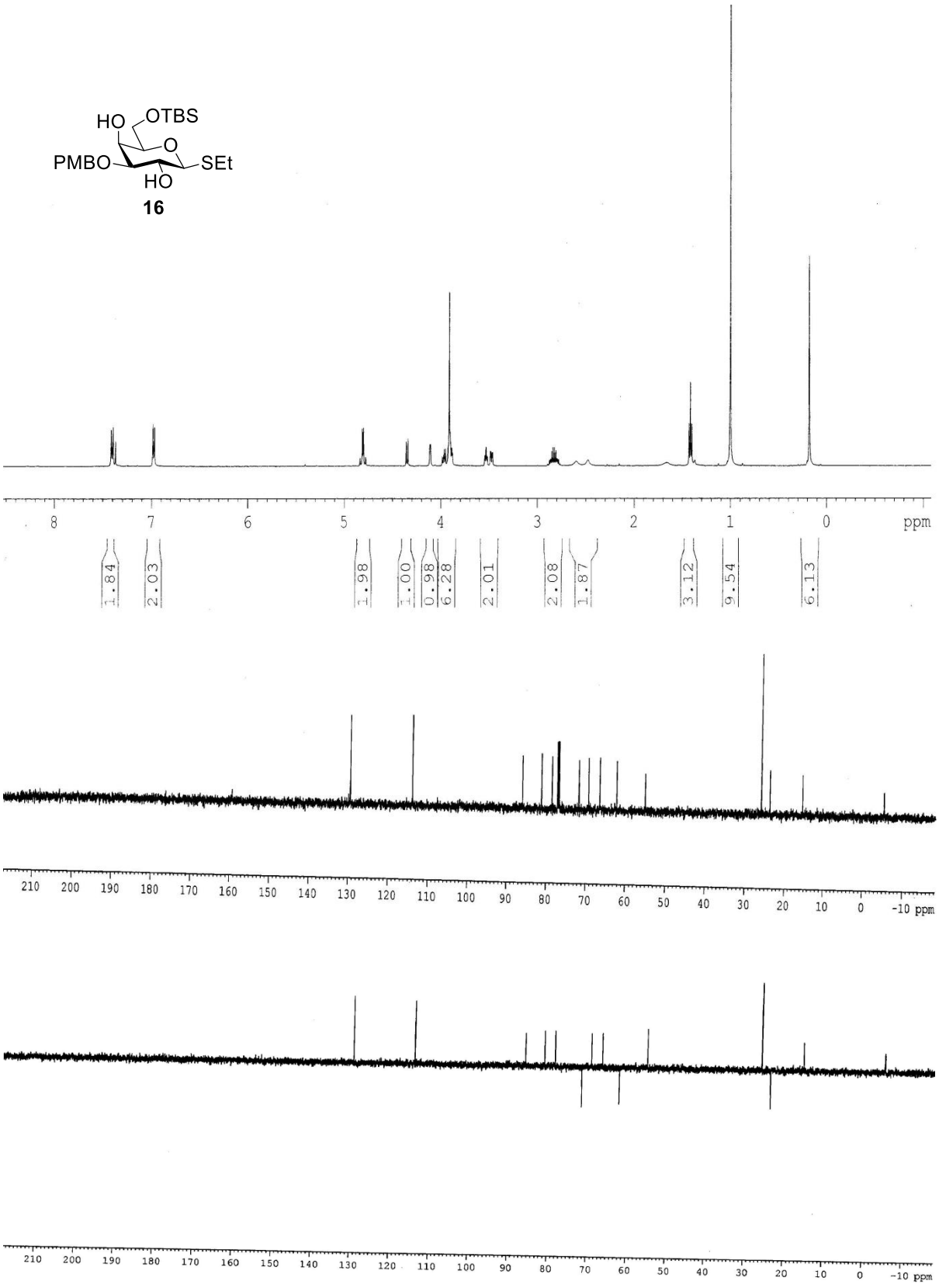

^{1}H, ^{13}C and DEPT-135 NMR spectra of ethyl 3-*O*-*p*-methoxybenzyl-6-*O*-(tert-butyldimethylsilyl)-1-thio-β-D-galactopyranoside(**16**)($CDCl_3$, 500 MHz).

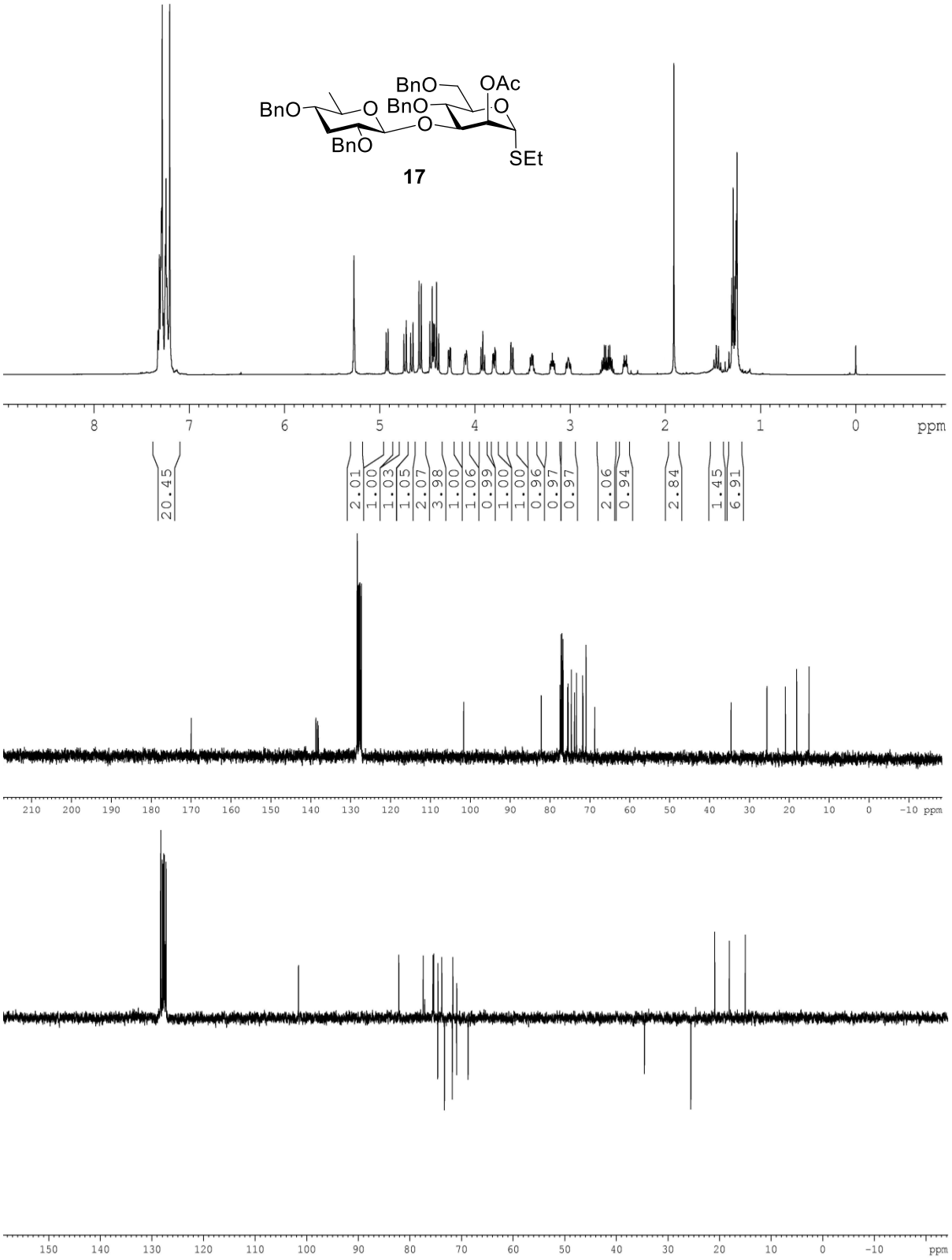

^{1}H, ^{13}C and DEPT-135 NMR spectra of ethyl (2,4-di-*O*-benzyl-3,6-dideoxy-β-D-ribo-hexopyranosyl)-(1→3)-2-*O*-acetyl-4,6-di-*O*-benzyl-1-thio-α-D-mannopyranoside (**17**) ($CDCl_3$, 500 MHz).

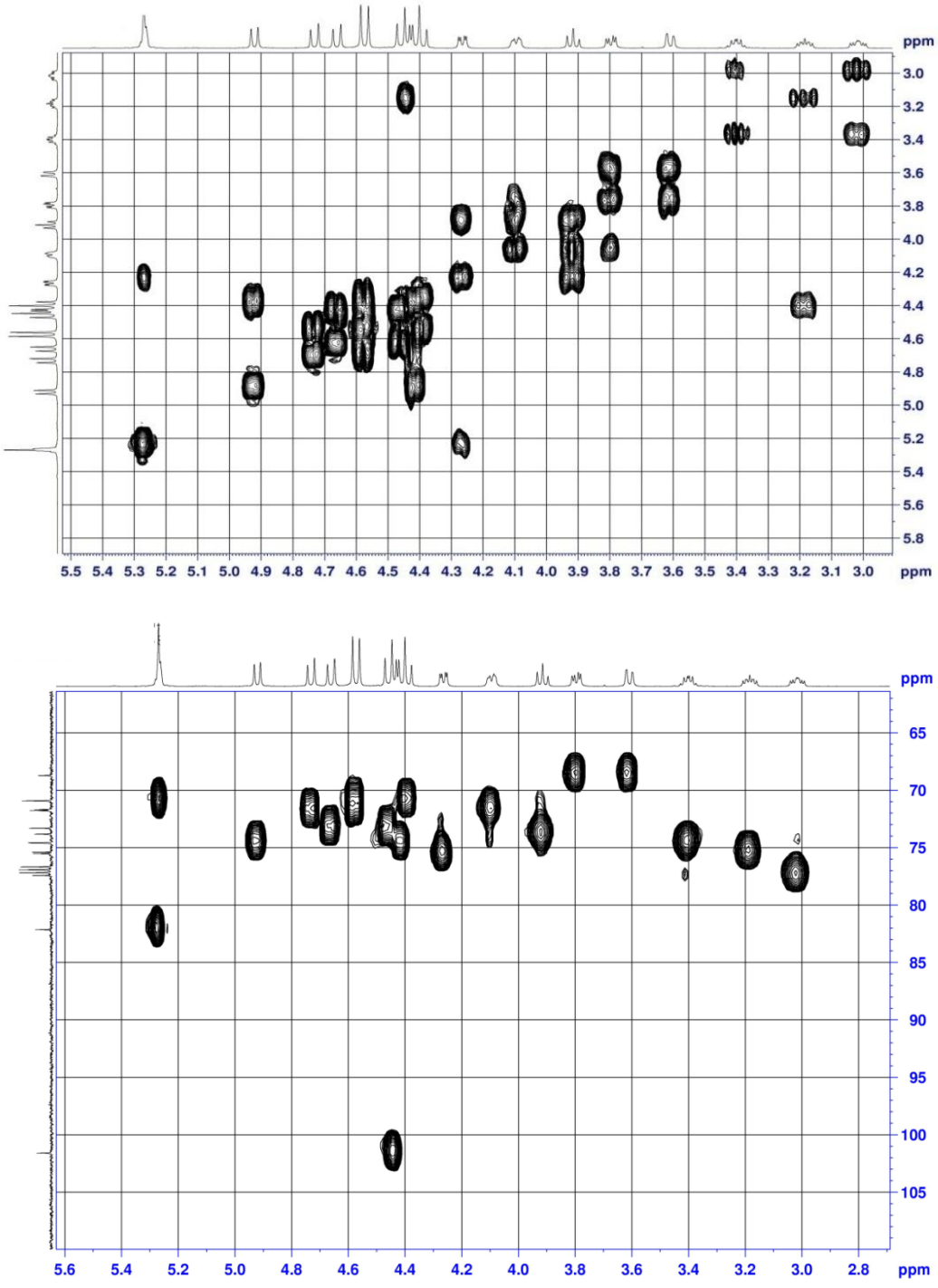

2D COSY and HMQC NMR spectra (selected regions) ofethyl (2,4-di-*O*-benzyl-3,6-dideoxy-β-D-ribo-hexopyranosyl)-(1→3)-2-*O*-acetyl-4,6-di-*O*-benzyl-1-thio-α-D-mannopyranoside (**17**) ($CDCl_3$, 500 MHz).

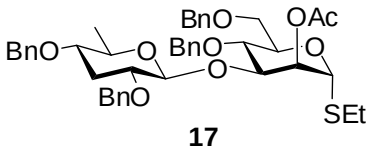

17

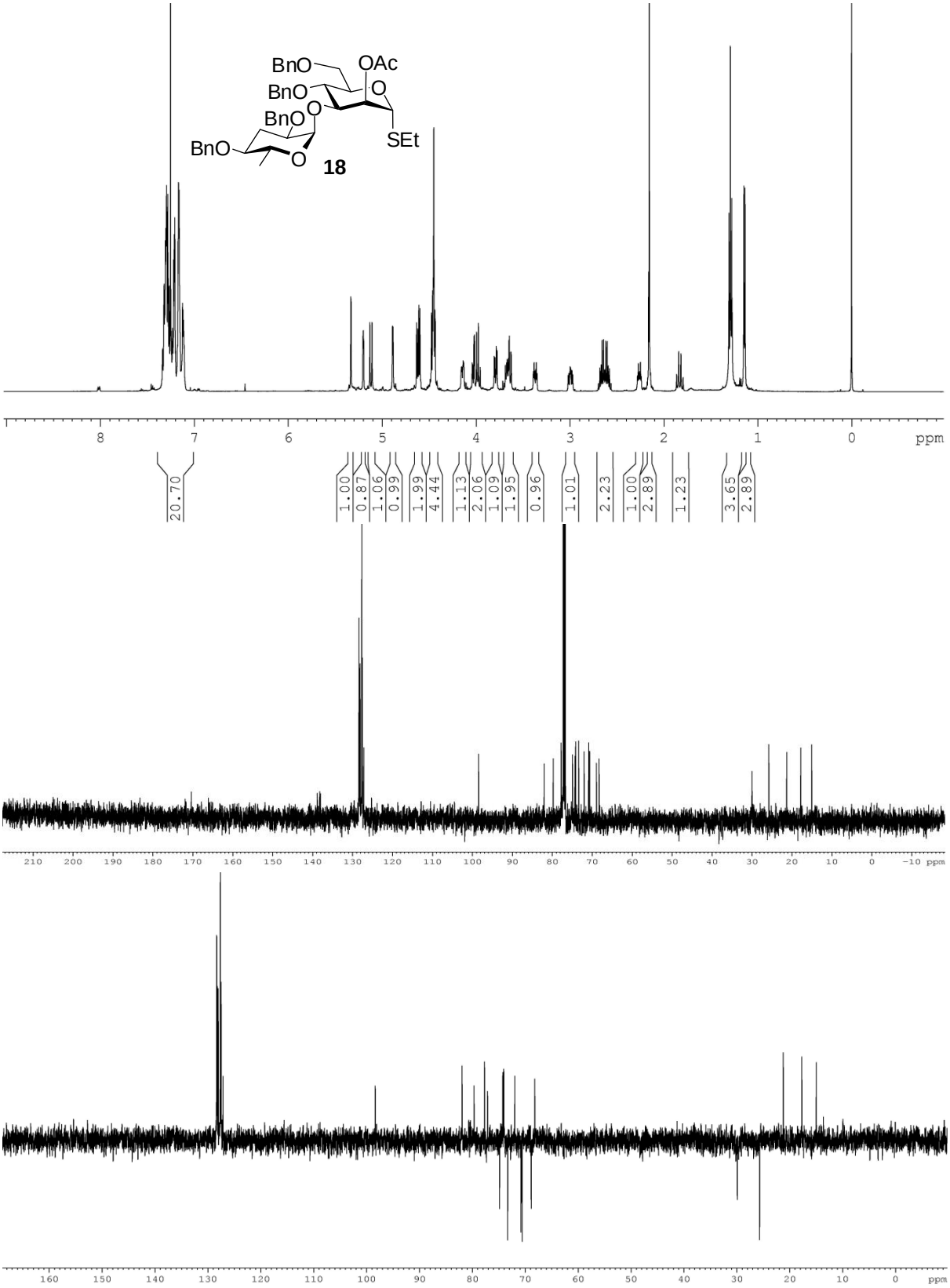

^{1}H, ^{13}C and DEPT-135 NMR spectra of ethyl (2,4-di-*O*-benzyl-3,6-dideoxy-α-D-ribo-hexopyranosyl)-(1→3)-2-*O*-acetyl-4,6-di-*O*-benzyl-1-thio-α-D-mannopyranoside (**18**) ($CDCl_3$, 500 MHz).

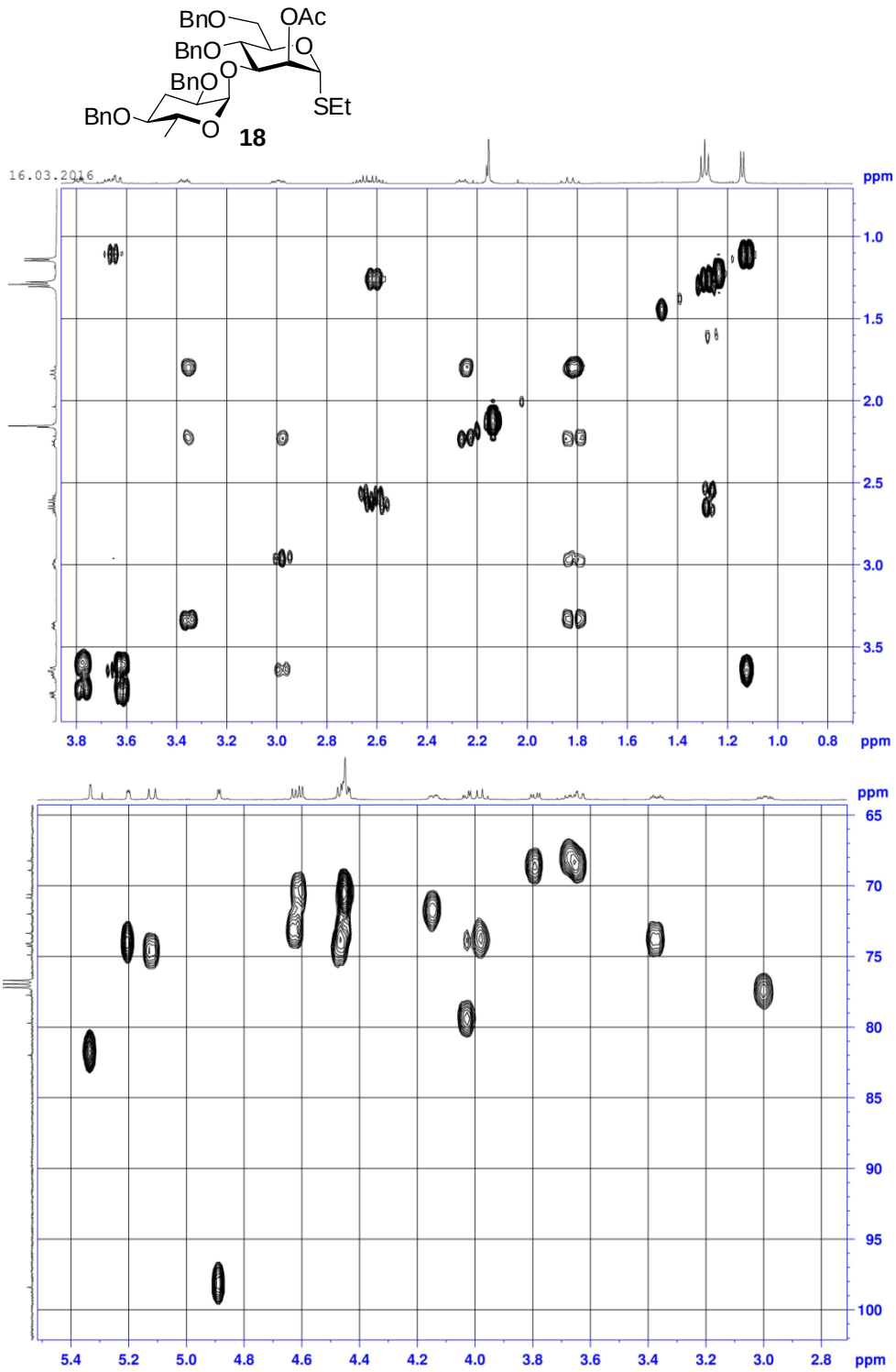

2D COSY and HMQC NMR spectra (selected regions) ofethyl (2,4-di-*O*-benzyl-3,6-dideoxy-α-D-ribo-hexopyranosyl)-(1→3)-2-*O*-acetyl-4,6-di-*O*-benzyl-1-thio-α-D-mannopyranoside (**18**) ($CDCl_3$, 500 MHz).

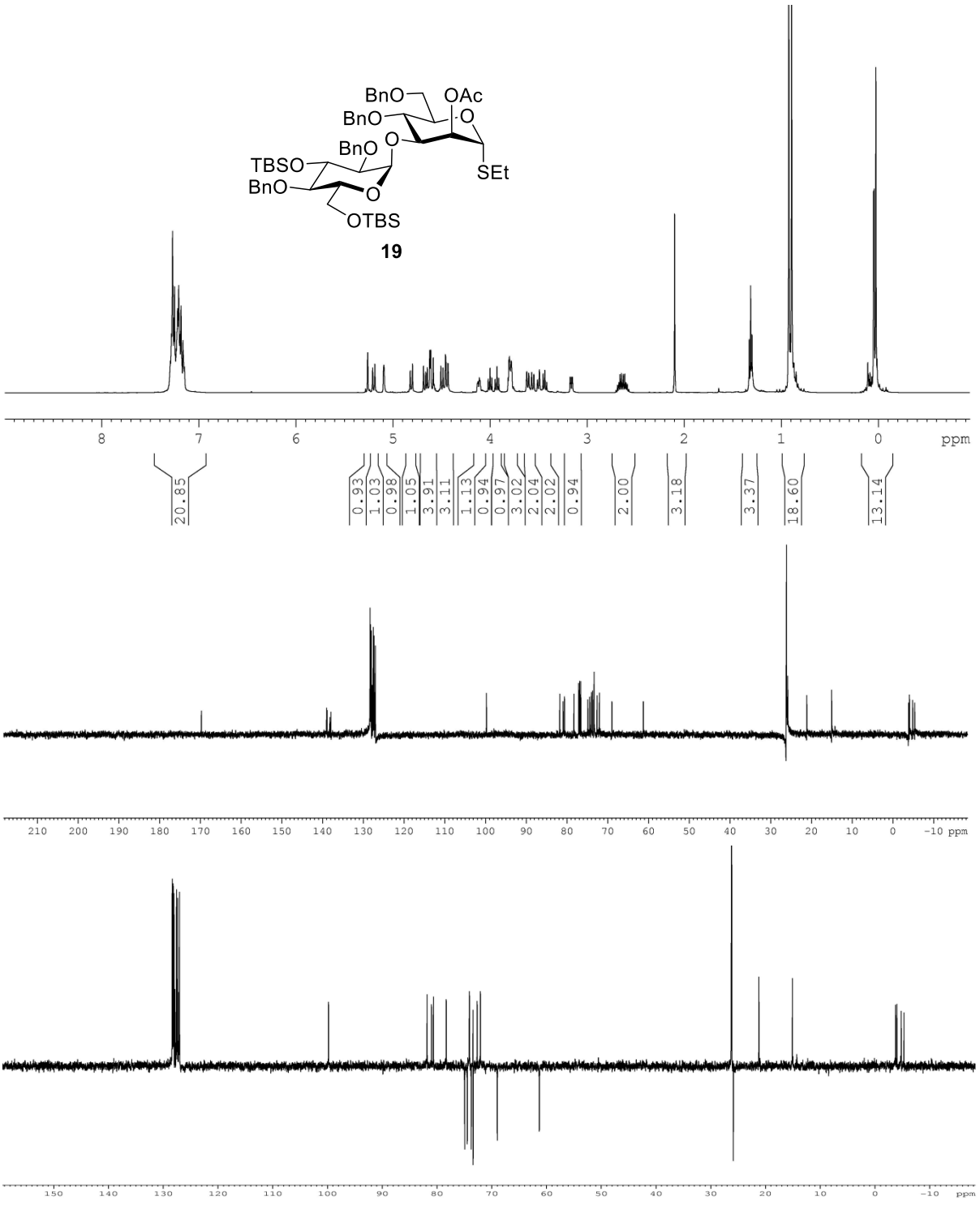

^{1}H, ^{13}C and DEPT-135 NMR spectra of ethyl (2,4-di-*O*-benzyl-3,6-di-*O*-(tert-butyldimethylsilyl)-α-D-glucopyranosyl)-(1→3)-2-*O*-acetyl-4,6-di-*O*-benzyl-1-thio-α-D-mannopyranoside (**19**)($CDCl_3$, 500 MHz).

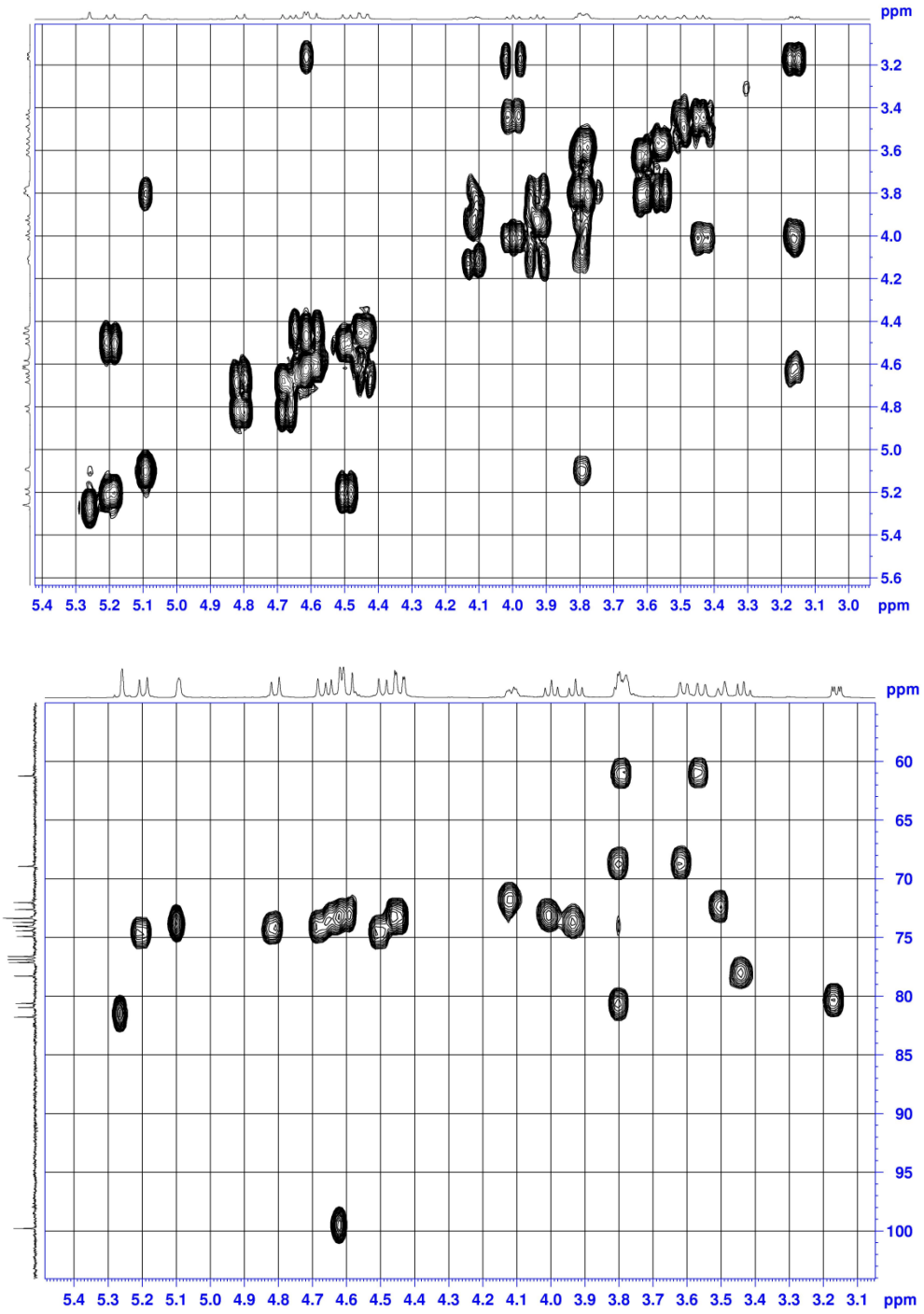

2D COSY and HSQC NMR spectra (selected regions) of ethyl (2,4-di-*O*-benzyl-3,6-di-*O*-(tert-butyldimethylsilyl)-α-D-glucopyranosyl)-(1→3)-2-*O*-acetyl-4,6-di-*O*-benzyl-1-thio-α-D-mannopyranoside (**19**)($CDCl_3$, 500 MHz).

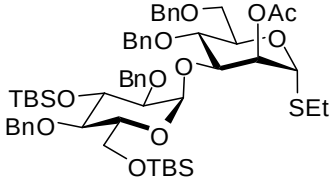

19

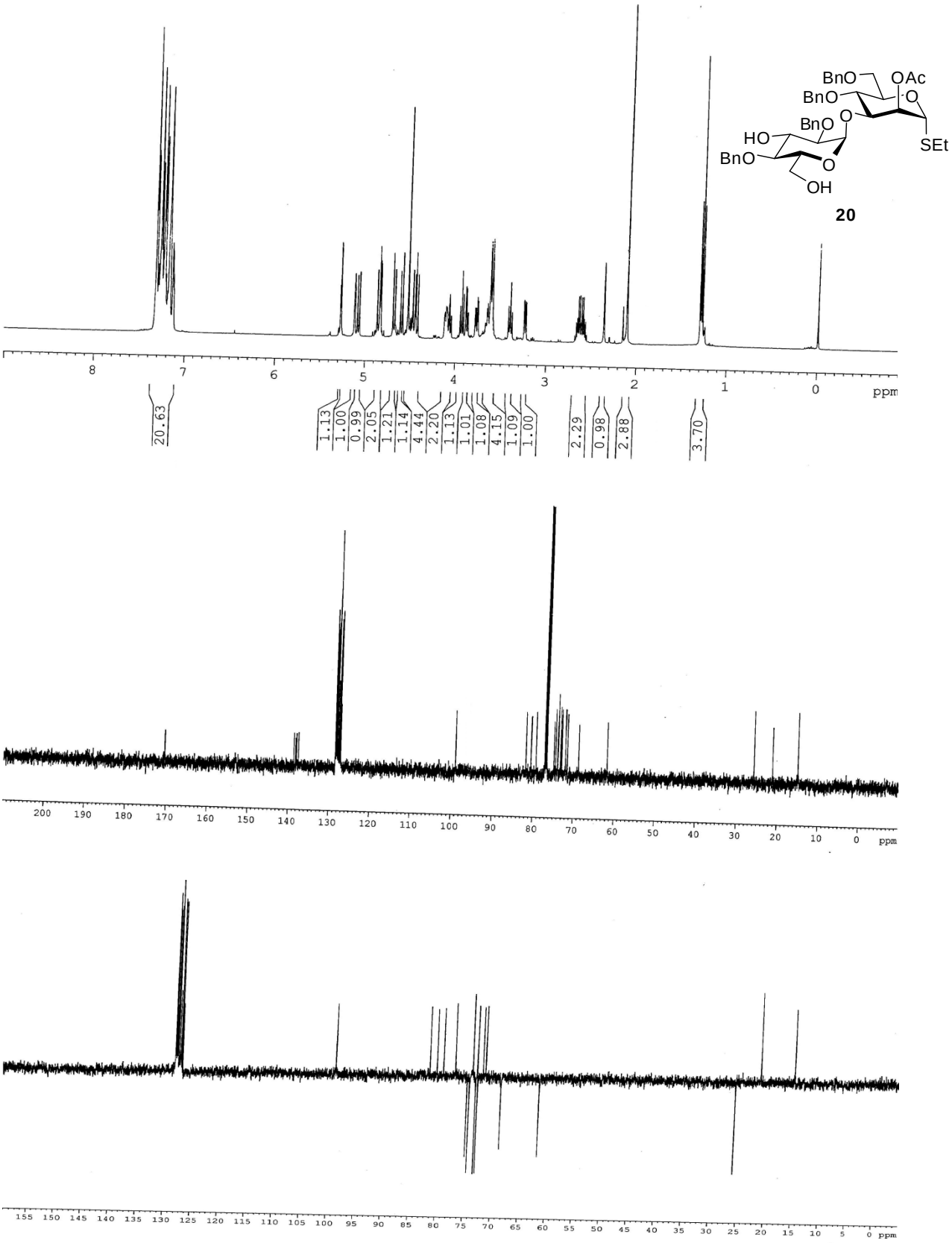

^{1}H, ^{13}C and DEPT-135 NMR spectra of ethyl (2,4-di-*O*-benzyl-α-D-glucopyranosyl)-(1→3)-2-*O*-acetyl-4,6-di-*O*-benzyl-1-thio-α-D-mannopyranoside (**20**)($CDCl_3$, 500 MHz).

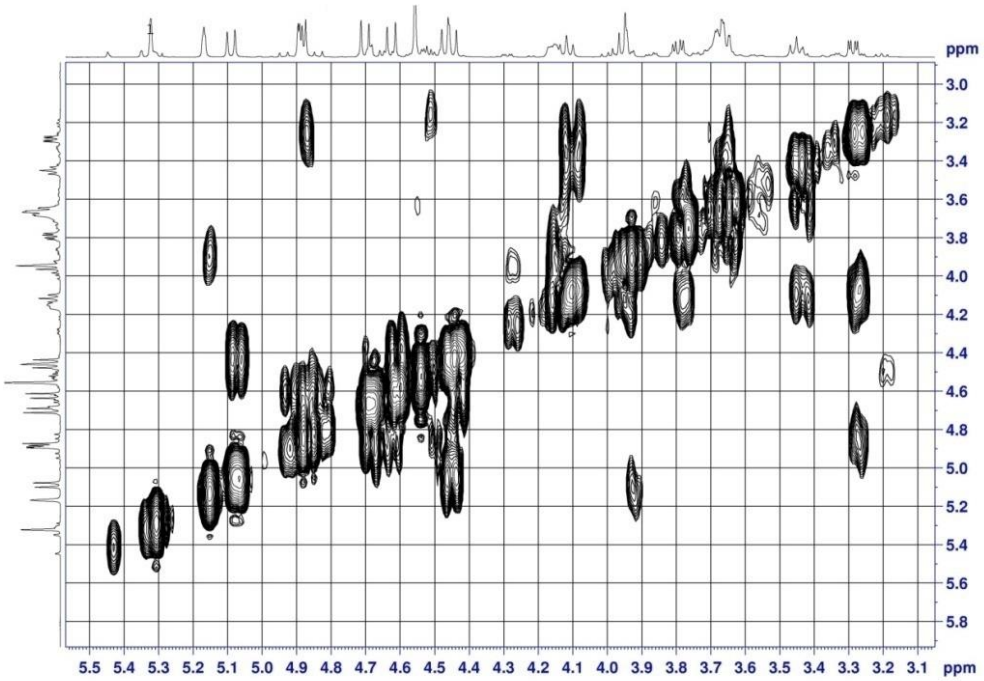

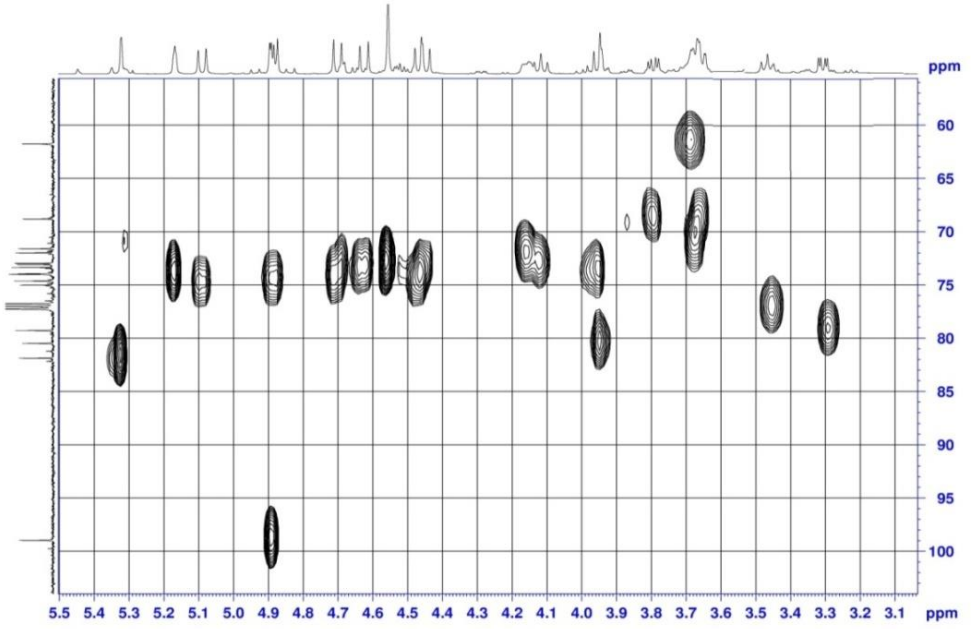

2D COSY and HSQC NMR spectra (selected regions) of ethyl (2,4-di-*O*-benzyl-α-D-glucopyranosyl)-(1→3)-2-*O*-acetyl-4,6-di-*O*-benzyl-1-thio-α-D-mannopyranoside (**20**)($CDCl_3$, 500 MHz).

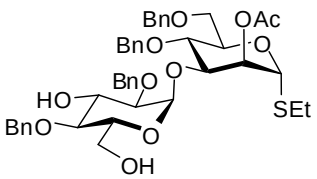

20

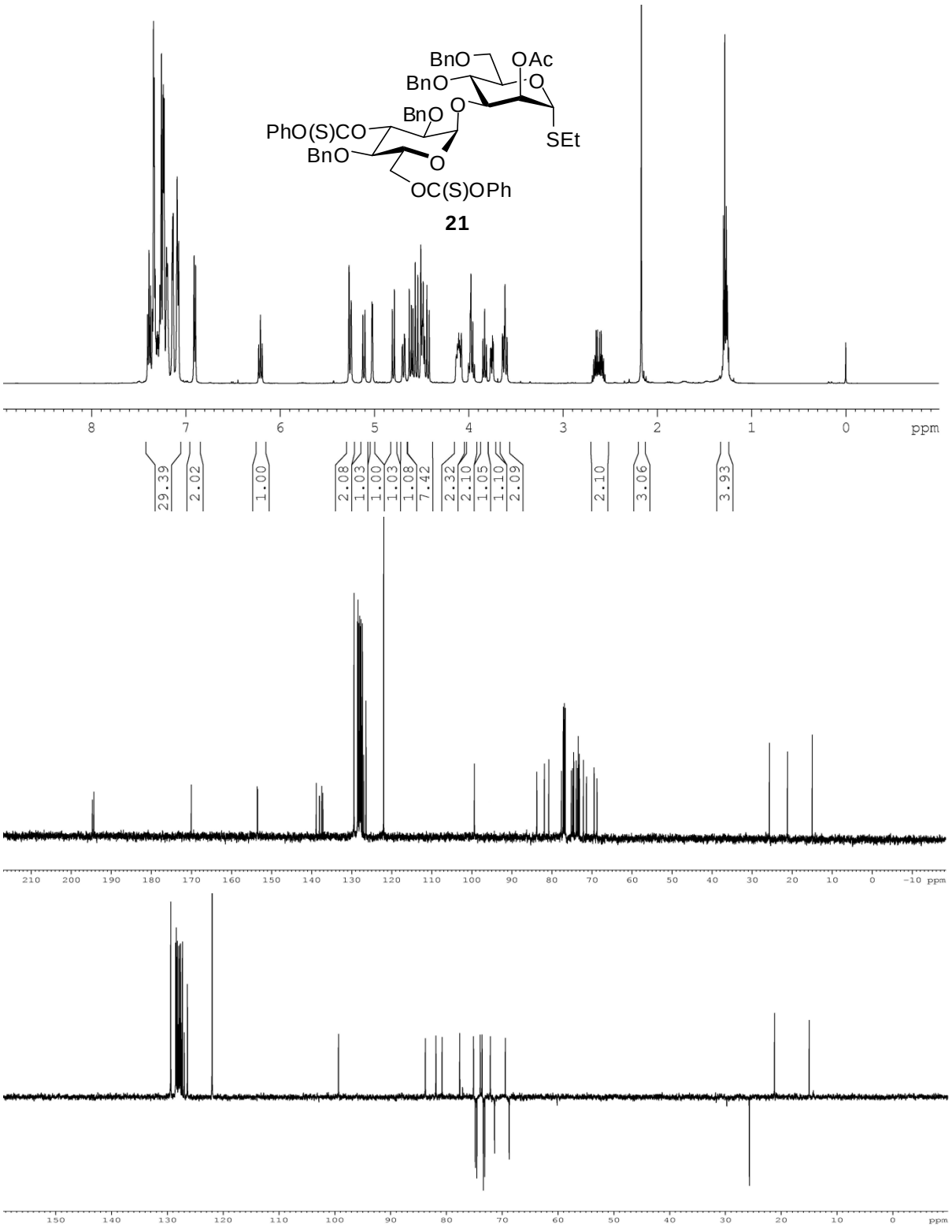

^{1}H, ^{13}C and DEPT-135 NMR spectra of ethyl (2,4-di-*O*-benzyl-3,6-di-phenoxythiocarbonyl-α-D-glucopyranosyl)-(1→3)-2-*O*-acetyl-4,6-di-*O*-benzyl-1-thio-α-D-mannopyranoside (**21**) ($CDCl_3$, 500 MHz).

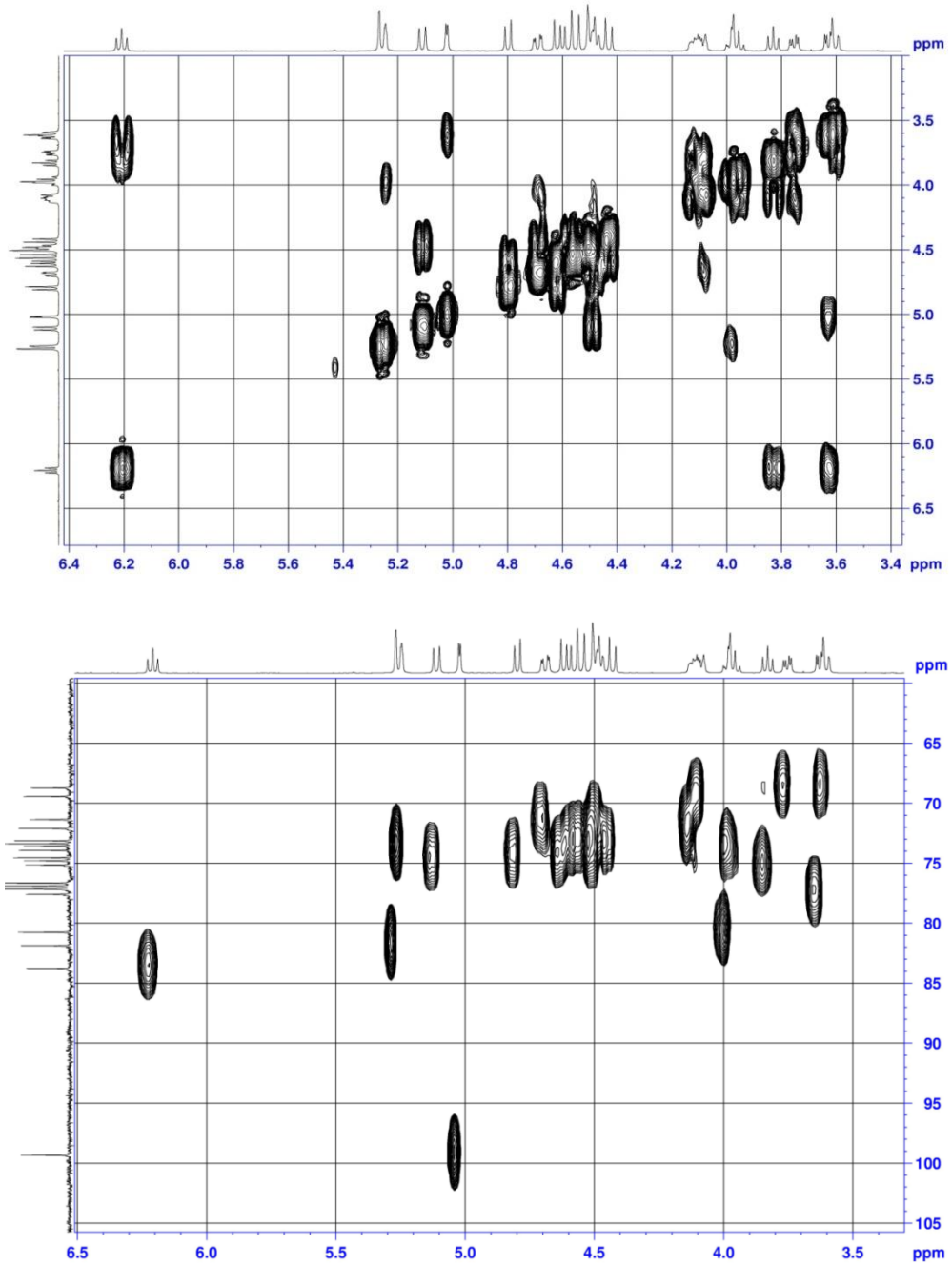

2D COSY and HSQC NMR spectra (selected regions) of ethyl (2,4-di-*O*-benzyl-3,6-di-phenoxythiocarbonyl-α-D-glucopyranosyl)-(1→3)-2-*O*-acetyl-4,6-di-*O*-benzyl-1-thio-α-D-mannopyranoside (**21)**($CDCl_3$, 500 MHz).

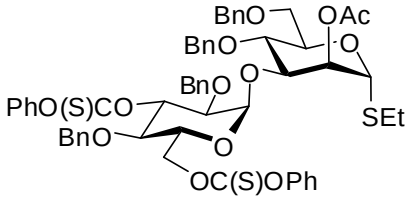

21

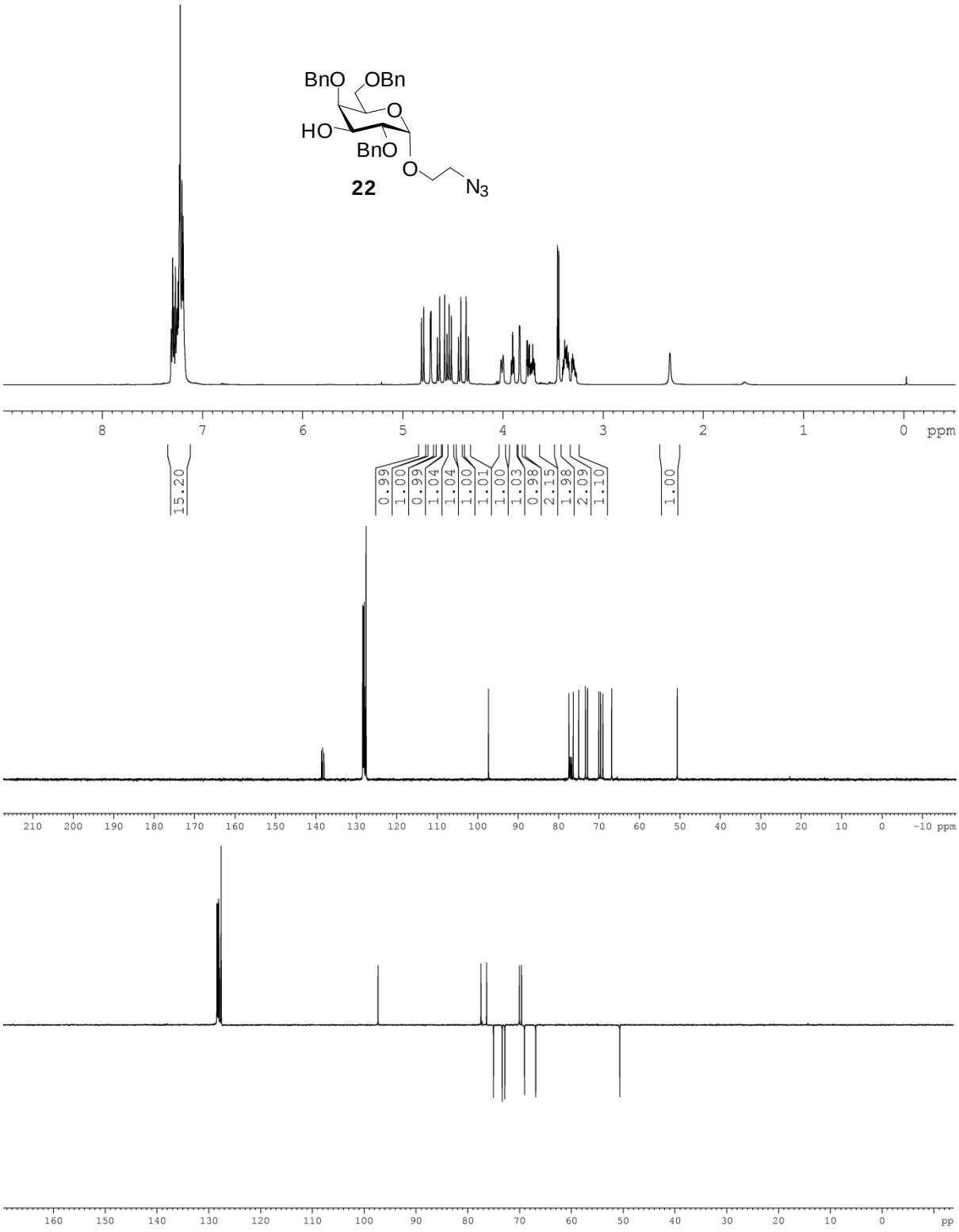

^{1}H, ^{13}C and DEPT-135 NMR spectra of 2-azidoethyl 2,4,6-tri-*O*-benzyl-α-D-galactopyranoside (**22**)($CDCl_3$, 500 MHz).

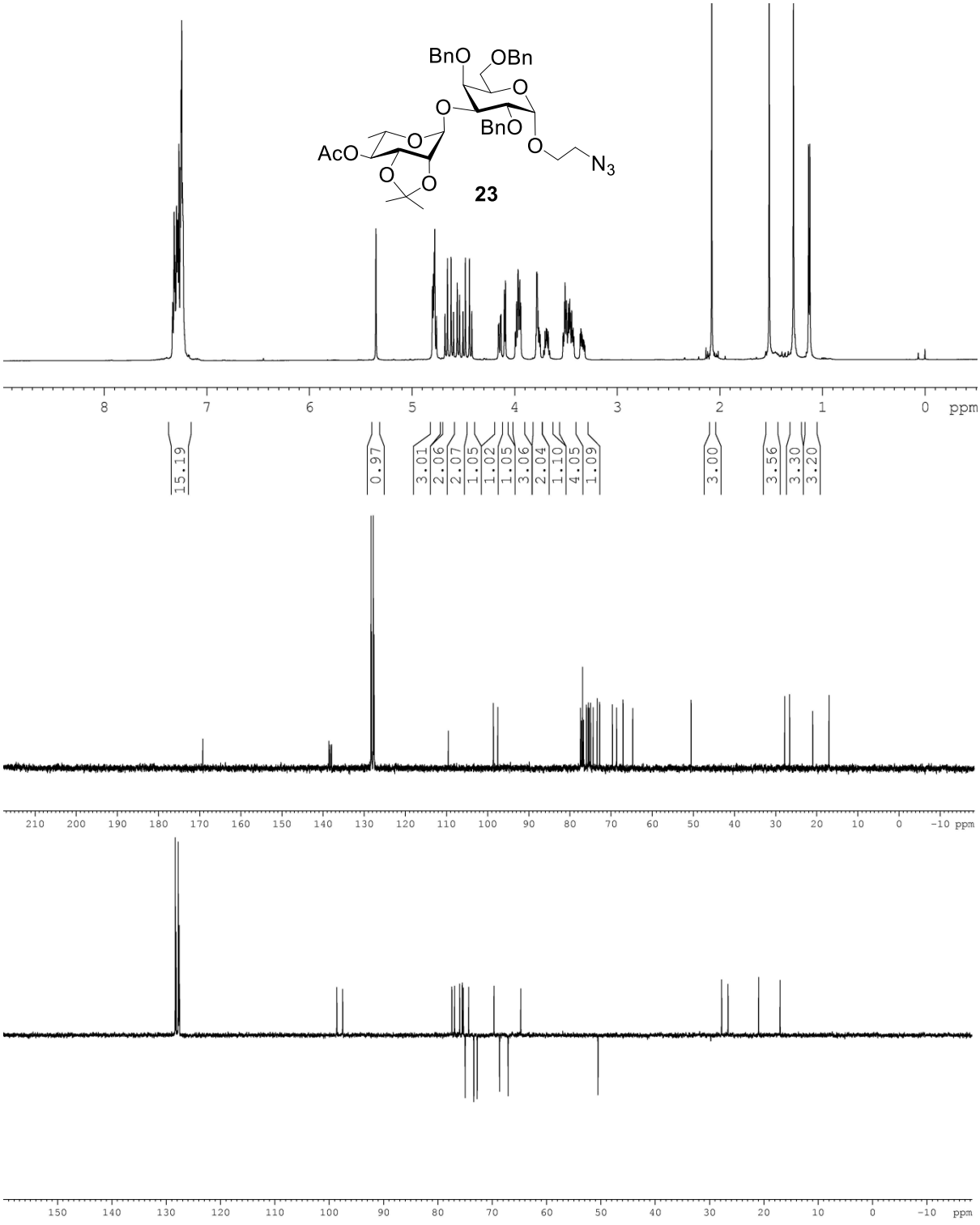

^{1}H, ^{13}C and DEPT-135 NMR spectra of 2-azidoethyl (4-*O*-acetyl-2,3-*O*-isopropylidene-α-L-rhamnopyranosyl)-(1→3)-2,4,6-tri-*O*-benzyl-α-D-galactopyranoside (**23**) ($CDCl_3$, 500 MHz).

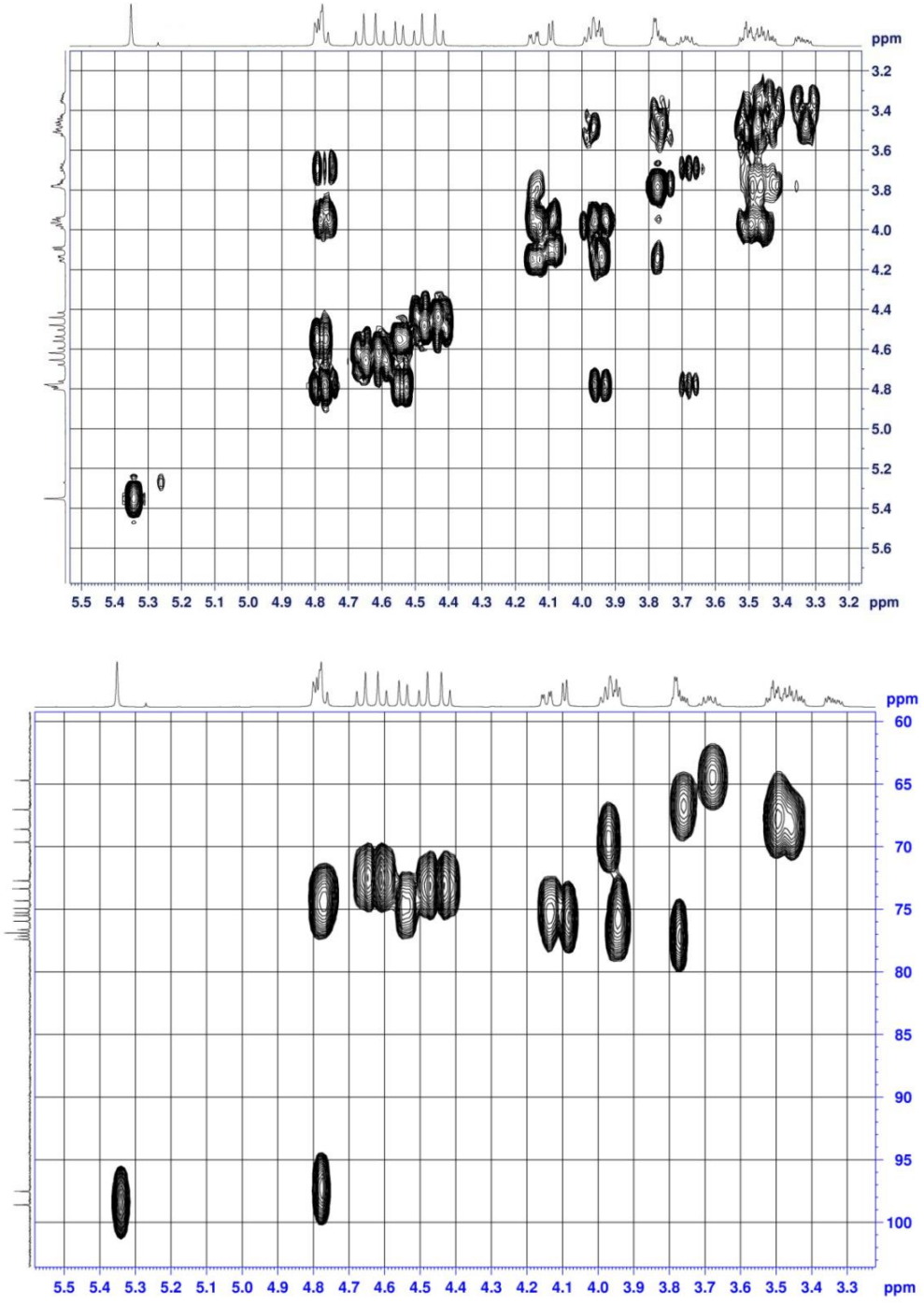

2D COSY and HSQC spectra (selected regions) of 2-azidoethyl (4-*O*-acetyl-2,3-*O*-isopropylidene-α-L-rhamnopyranosyl)-(1→3)-2,4,6-tri-*O*-benzyl-α-D-galactopyranoside (**23**) ($CDCl_3$, 500 MHz).

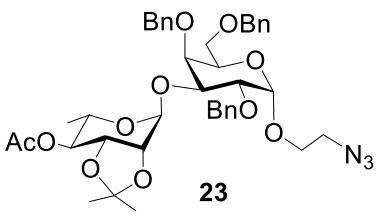

23

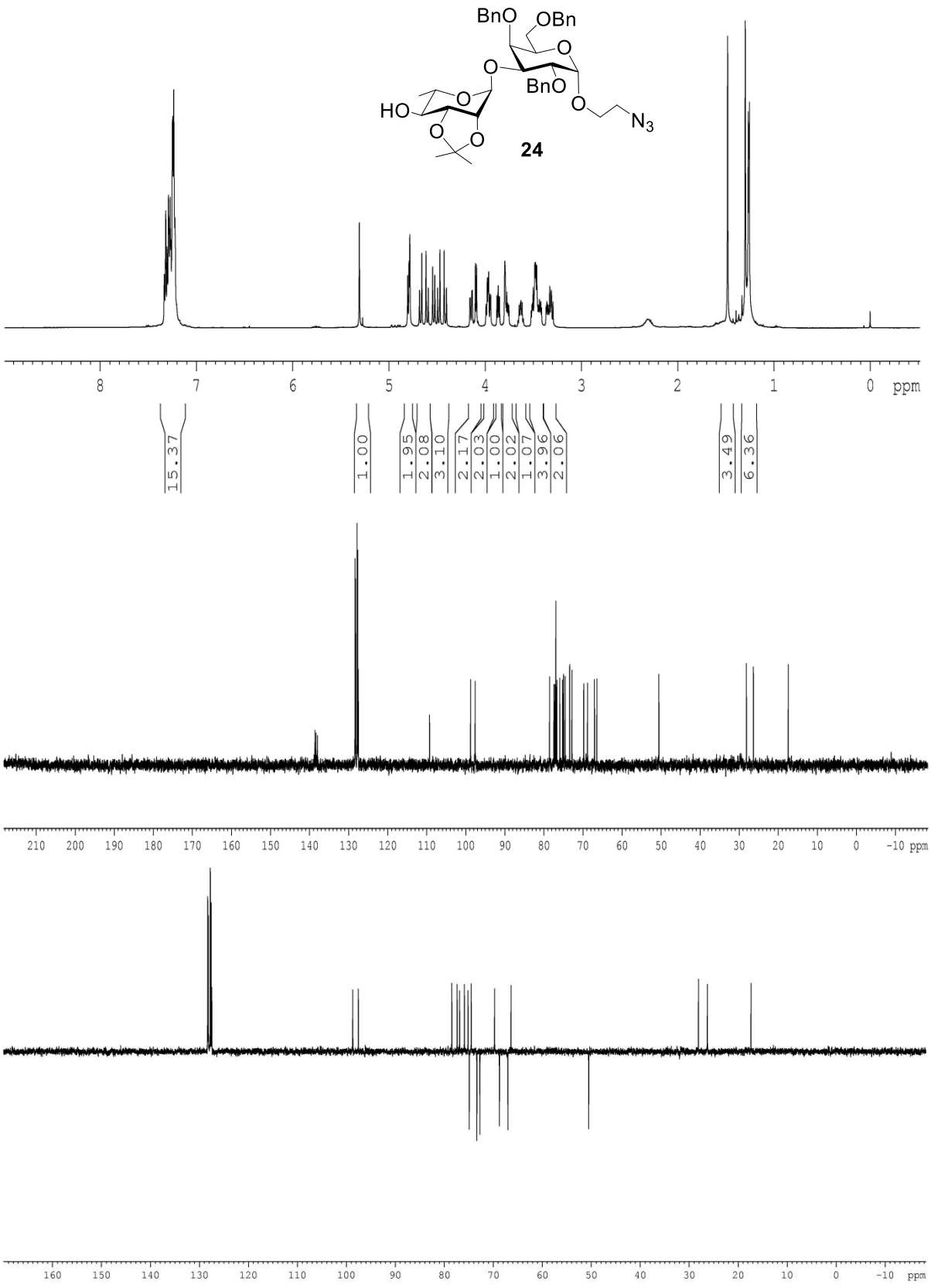

^{1}H, ^{13}C and DEPT-135 NMR spectra of 2-azidoethyl (2,3-*O*-isopropylidene-α-L-rhamnopyranosyl)-(1→3)-2,4,6-tri-*O*-benzyl-α-D-galactopyranoside (**24**) ($CDCl_3$, 500 MHz).

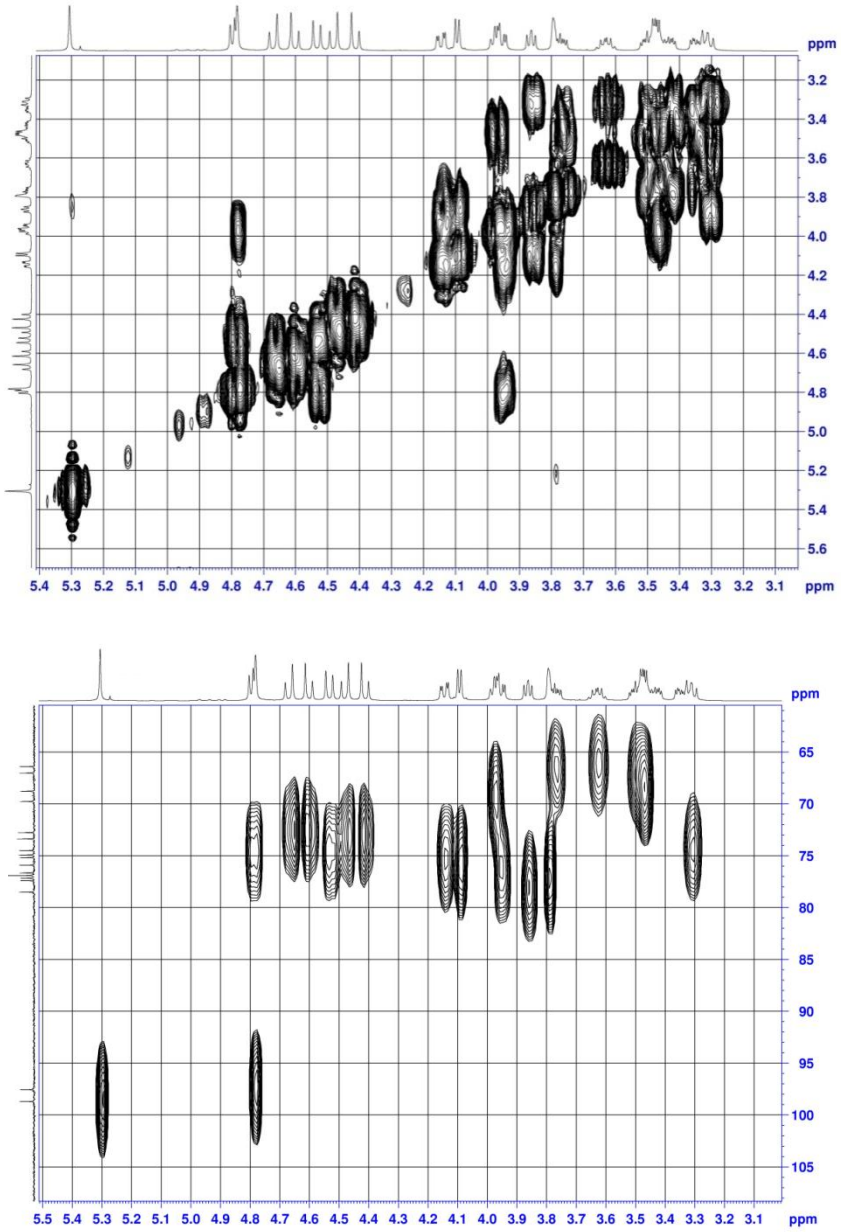

2D COSY and HSQC NMR spectra (selected regions) of 2-azidoethyl (2,3-*O*-isopropylidene-α-L-rhamnopyranosyl)-(1→3)-2,4,6-tri-*O*-benzyl-α-D-galactopyranoside (**24**) ($CDCl_3$, 500 MHz).

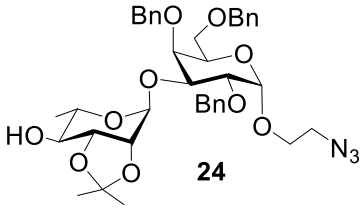

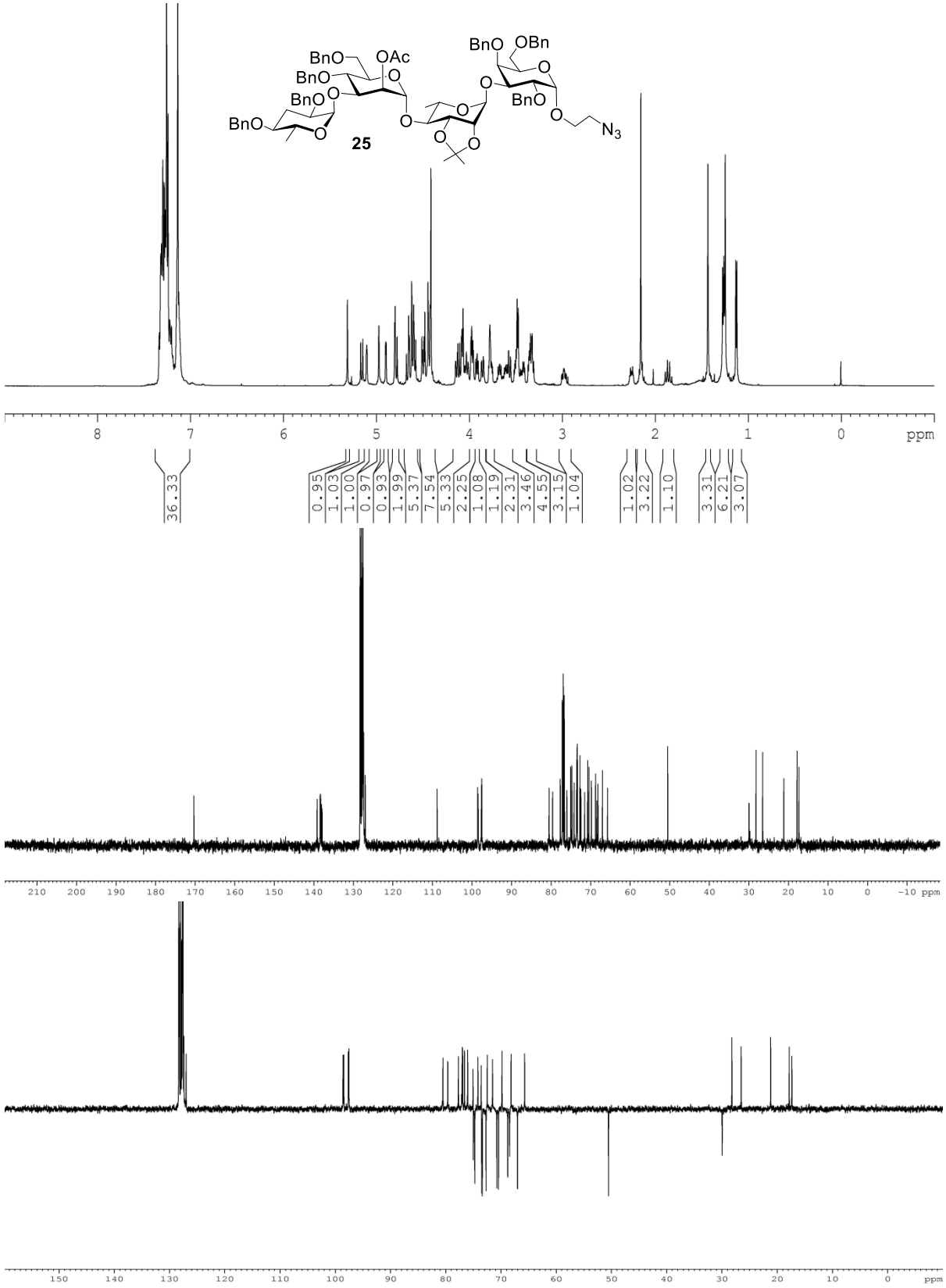

^{1}H, ^{13}C and DEPT-135 NMR spectra of 2-azidoethyl (2,4-di-*O*-benzyl-3,6-dideoxy-α-D-ribo-hexopyranosyl)-(1→3)-(2-*O*-acetyl-4,6-di-*O*-benzyl-α-D-mannopyranosyl)-(1→4)-(2,3-*O*-isopropylidene-α-L-rhamnopyranosyl)-(1→3)-2,4,6-tri-*O*-benzyl-α-D-galactopyranoside (**25**) ($CDCl_3$, 500 MHz).

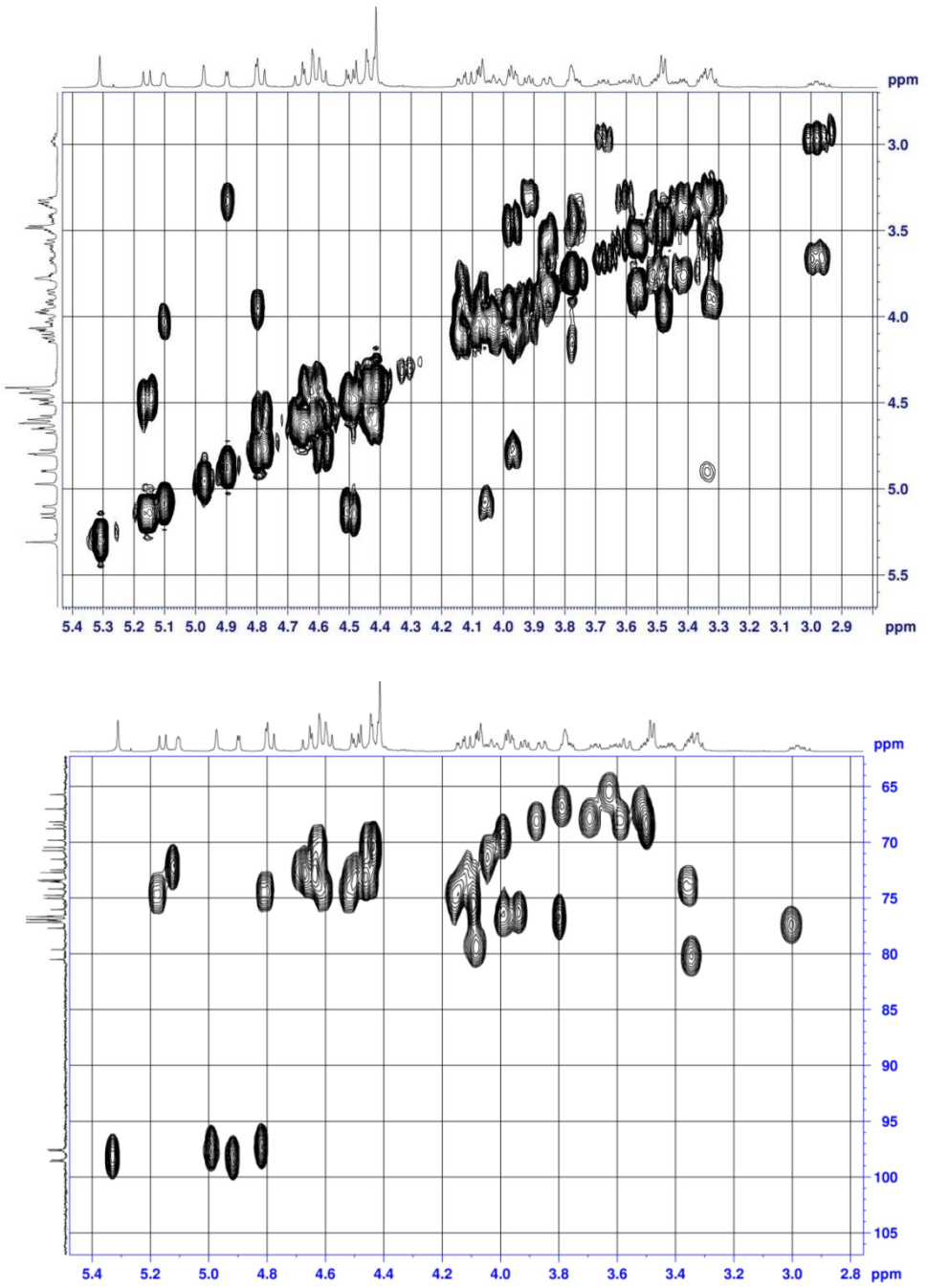

2D COSY and HSQC NMR spectra (selected regions) of 2-azidoethyl (2,4-di-*O*-benzyl-3,6-dideoxy-α-D-ribo-hexopyranosyl)-(1→3)-(2-*O*-acetyl-4,6-di-*O*-benzyl-α-D-mannopyranosyl)-(1→4)-(2,3-*O*-isopropylidene-α-L-rhamnopyranosyl)-(1→3)-2,4,6-tri-*O*-benzyl-α-D-galactopyranoside (**25**) ($CDCl_3$, 500 MHz).

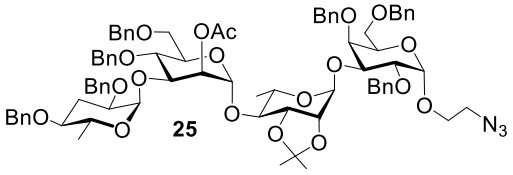

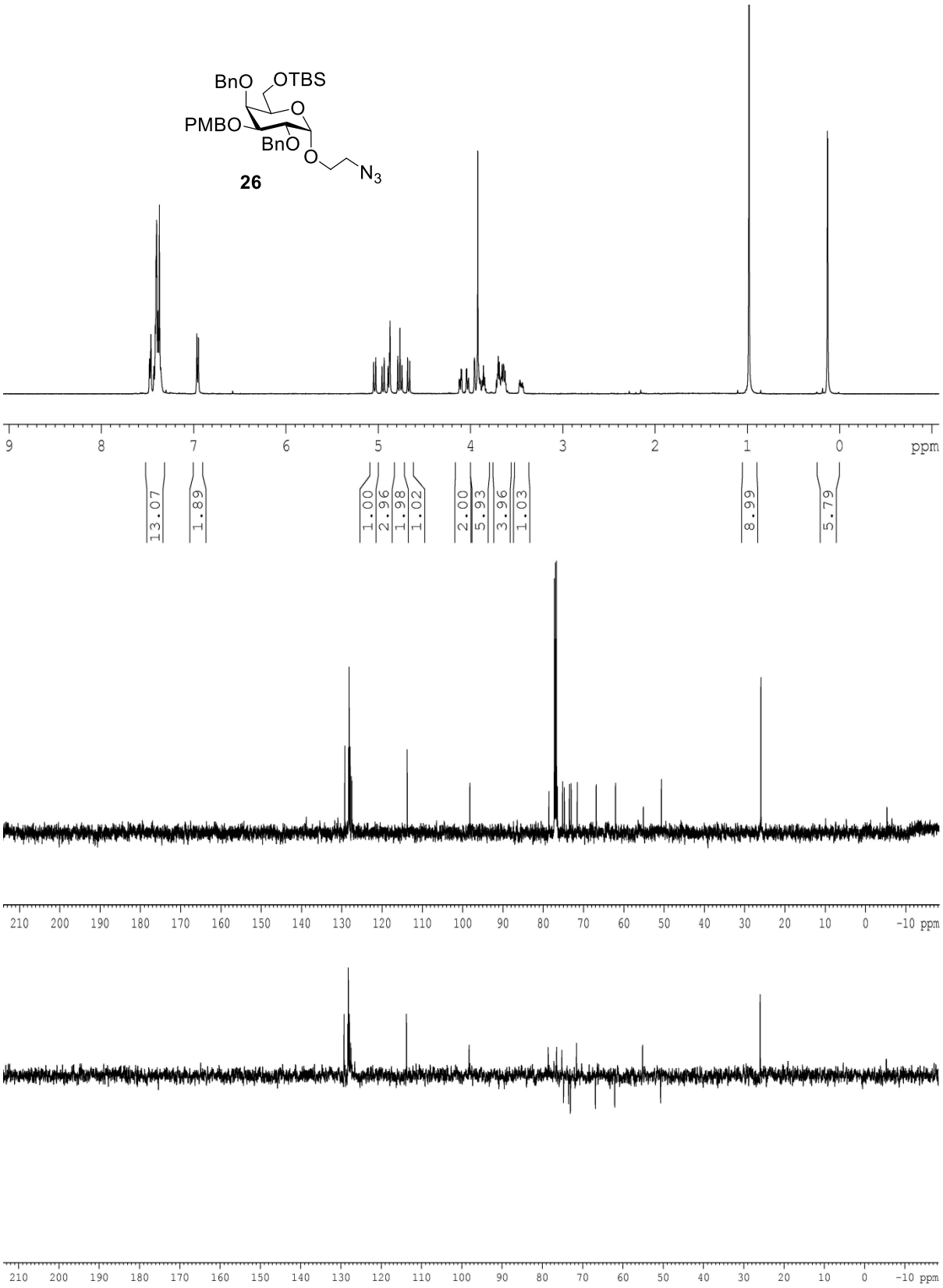

^{1}H, ^{13}C and DEPT-135 spectra of 2-azidoethyl 2,4-di-*O*-benzyl-3-*O*-p-methoxybenzyl-6-*O*-(*tert*-butyldimethylsilyl)-α-D-galactopyranoside (**26**)($CDCl_3$, 500 MHz).

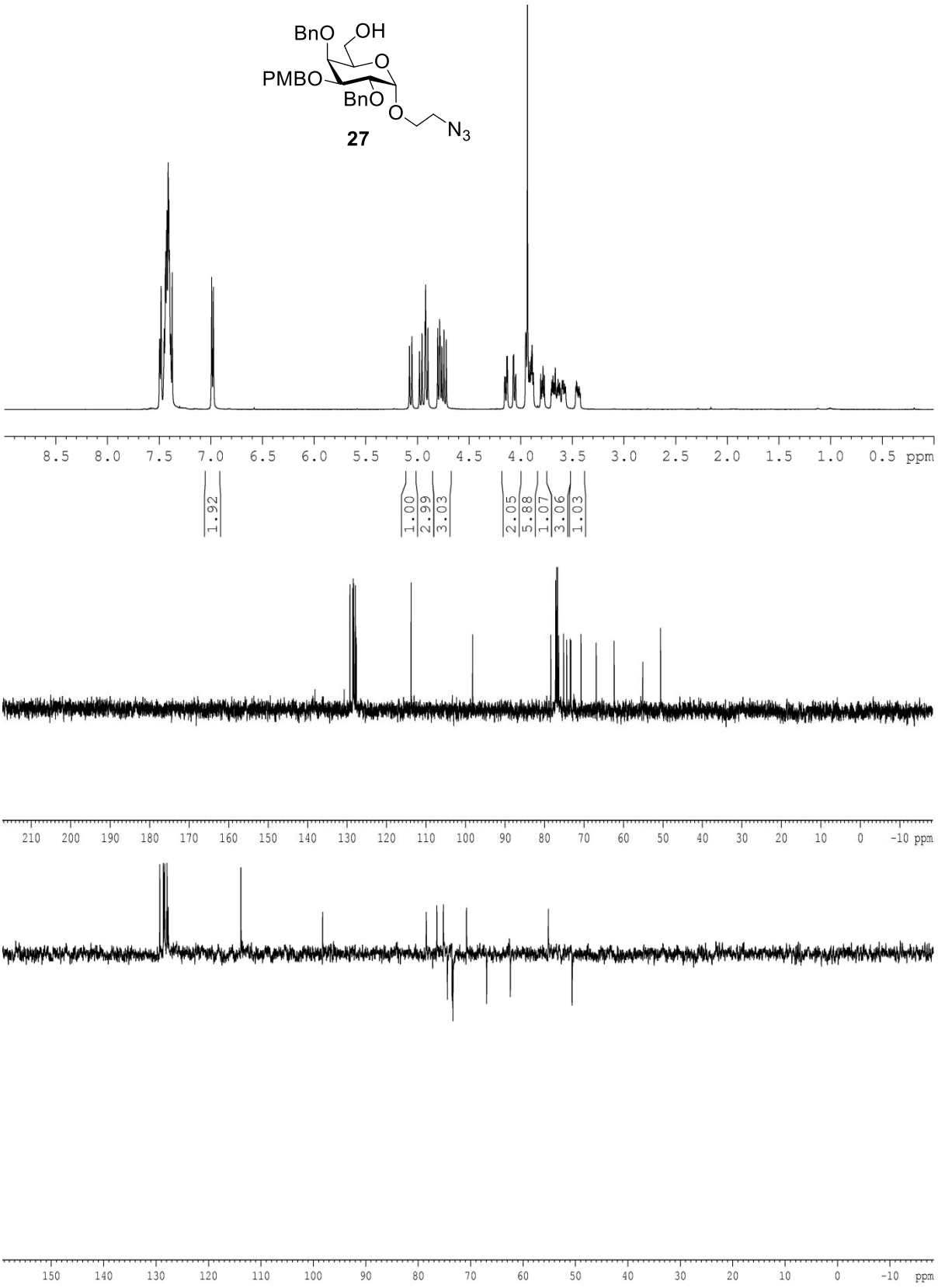

^{1}H, ^{13}C and DEPT-135 spectra of 2-azidoethyl 2,4-di-*O*-benzyl-3-*O*-*p*-methoxybenzyl-α-D-galactopyranoside (**27**)($CDCl_3$, 500 MHz).

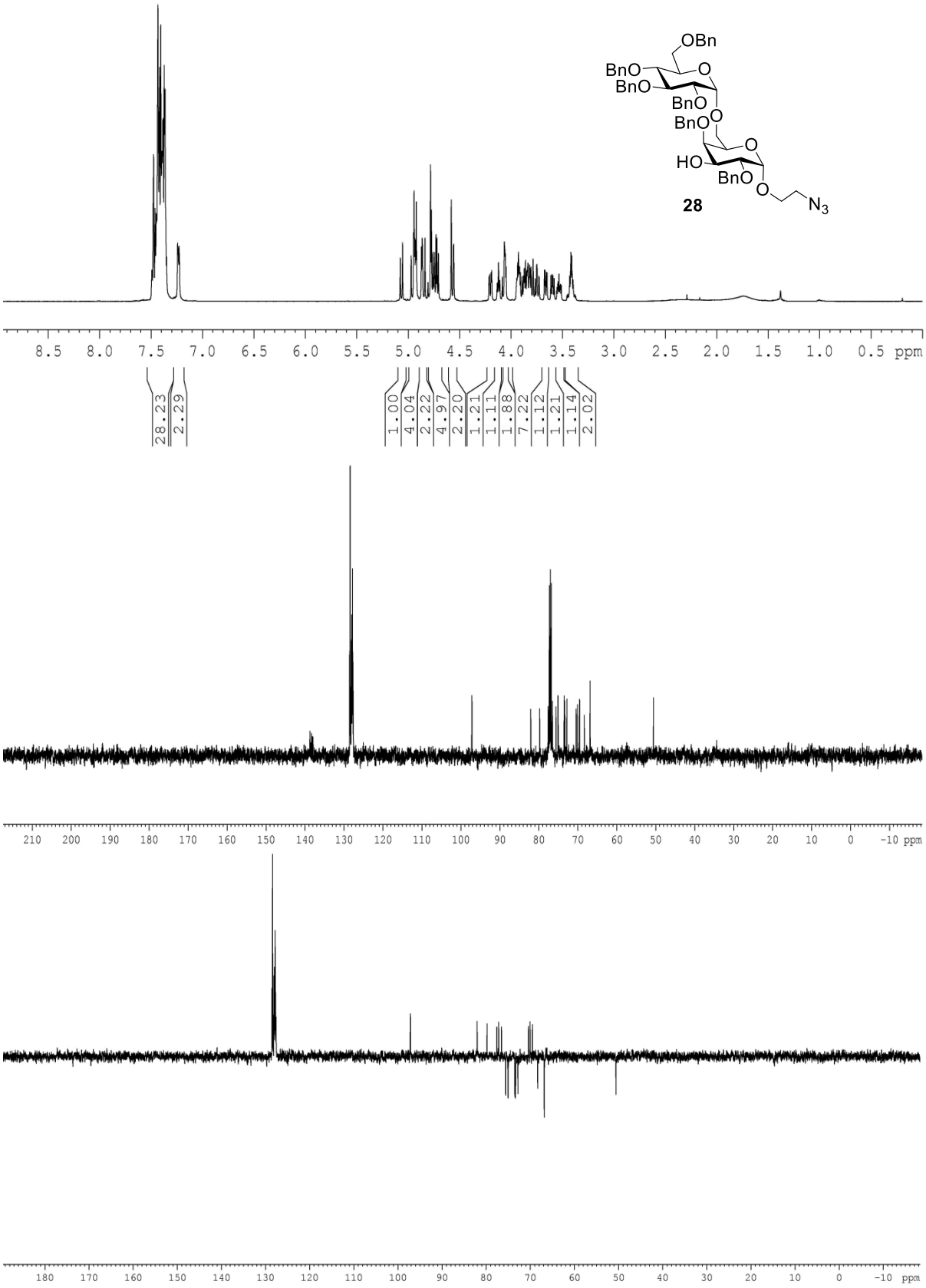

^{1}H, ^{13}C and DEPT-135 spectra of 2-azidoethyl (2,3,4,6-tetra-*O*-benzyl-α-D-glucopyranosyl)-(1→6)-2,4-di-*O*-benzyl-α-D-galactopyranoside (**28**)($CDCl_3$, 500 MHz).

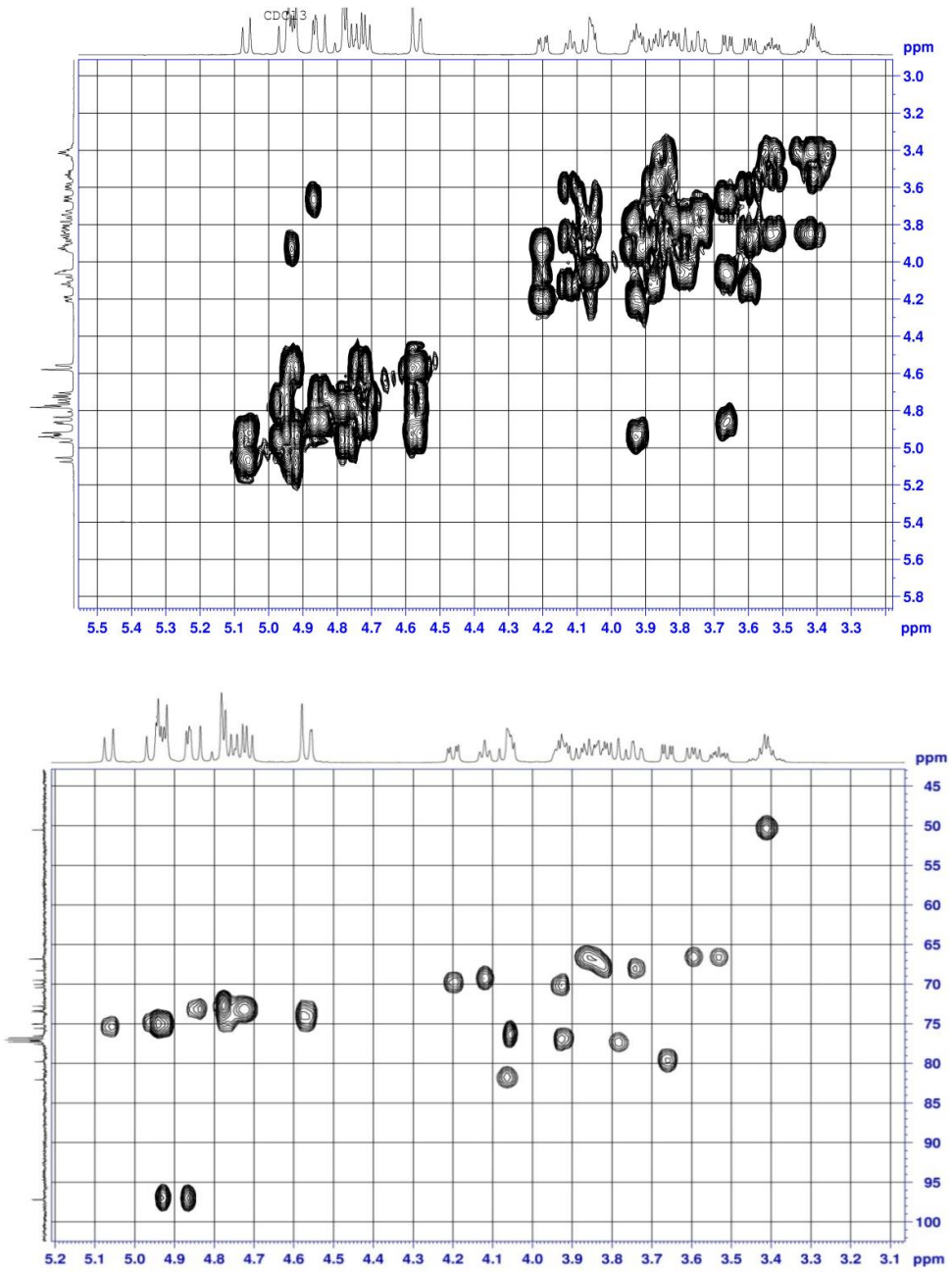

2D COSY and HSQC NMR spectra (selected regions) of 2-azidoethyl (2,3,4,6-tetra-*O*-benzyl-α-D-glucopyranosyl)-(1→6)-2,4-di-*O*-benzyl-α-D-galactopyranoside (**28**)($CDCl_3$, 500 MHz).

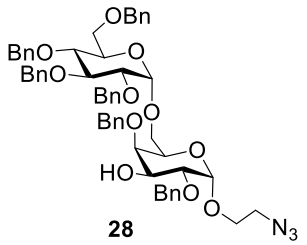

28

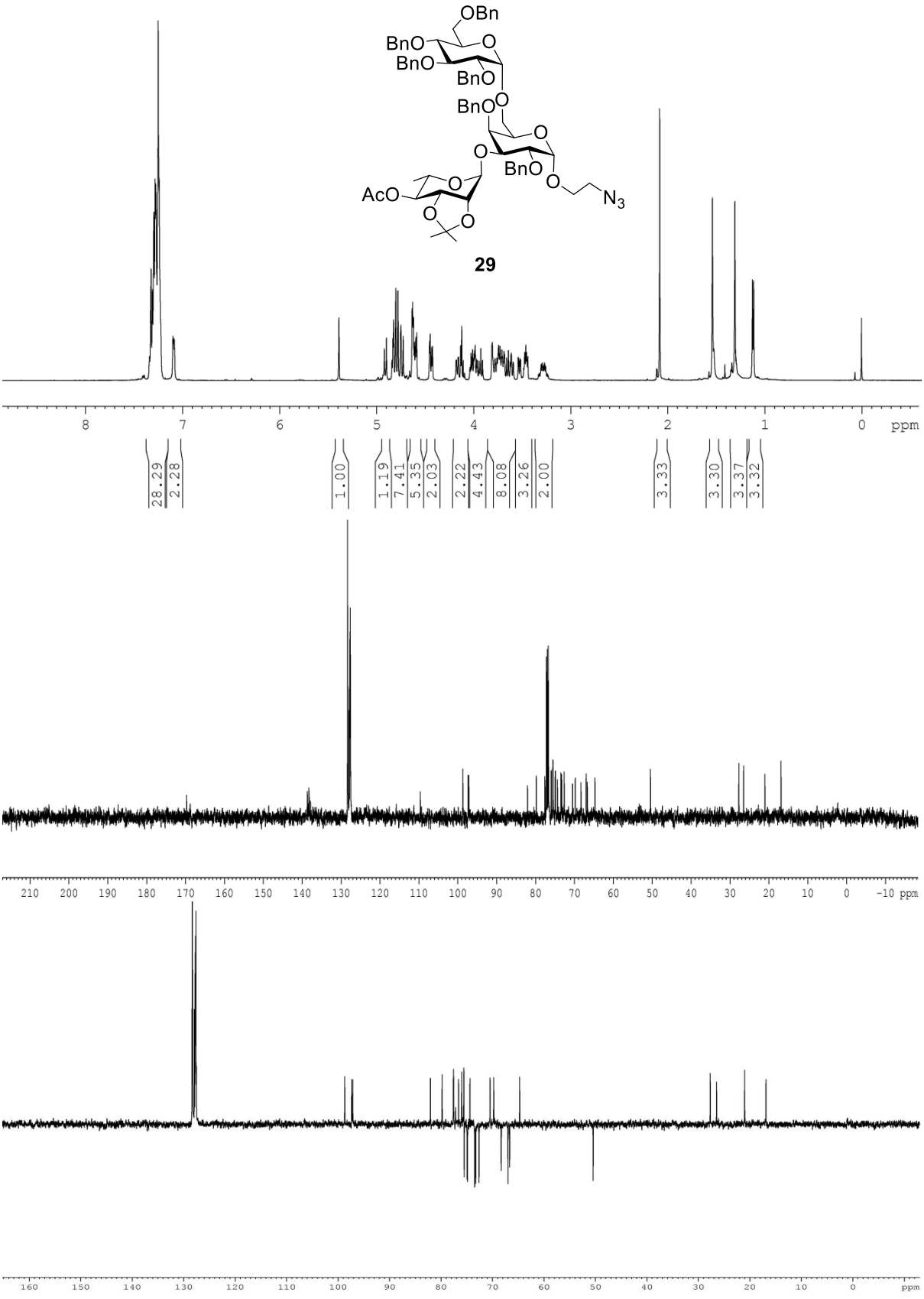

^{1}H, ^{13}C and DEPT-135 NMR spectra of 2-azidoethyl (4-*O*-acetyl-2,3-*O*-isopropylidene-α-L-rhamnopyranosyl)-(1→3)-[(2,3,4,6-tetra-*O*-benzyl-α-D-glucopyranosyl)-(1→6)]-2,4-di-*O*-benzyl-α-D-galactopyranoside (**29**) ($CDCl_3$, 500 MHz).

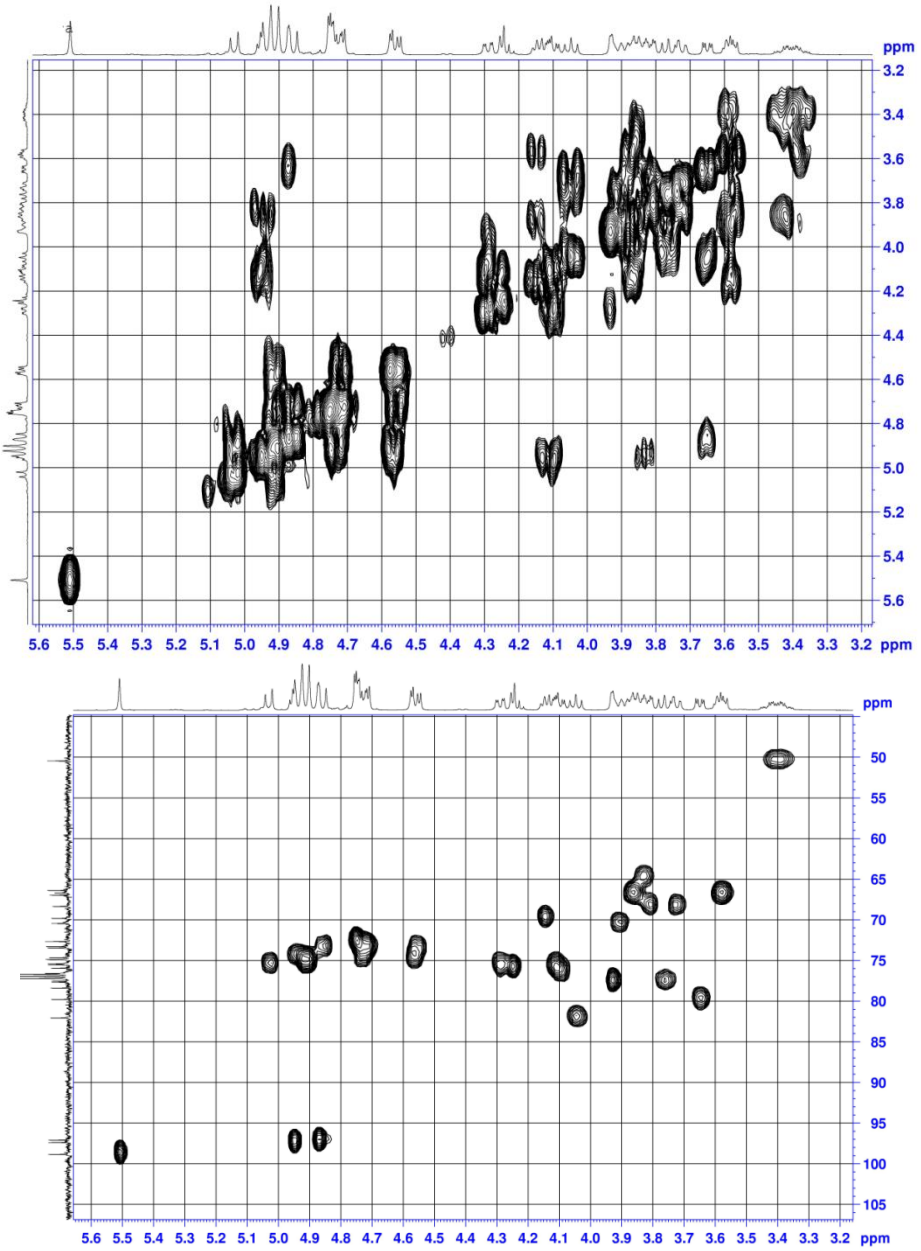

2D COSY and HSQC NMR spectra (selected regions) of 2-azidoethyl (4-*O*-acetyl-2,3-*O*-isopropylidene-α-L-rhamnopyranosyl)-(1→3)-[(2,3,4,6-tetra-*O*-benzyl-α-D-glucopyranosyl)-(1→6)]-2,4-di-*O*-benzyl-α-D-galactopyranoside (**29**) ($CDCl_3$, 500 MHz).

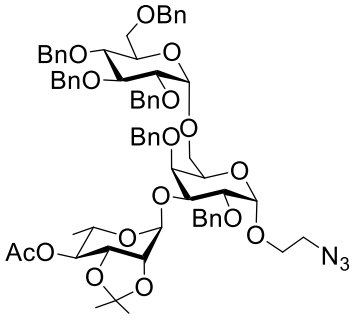

29

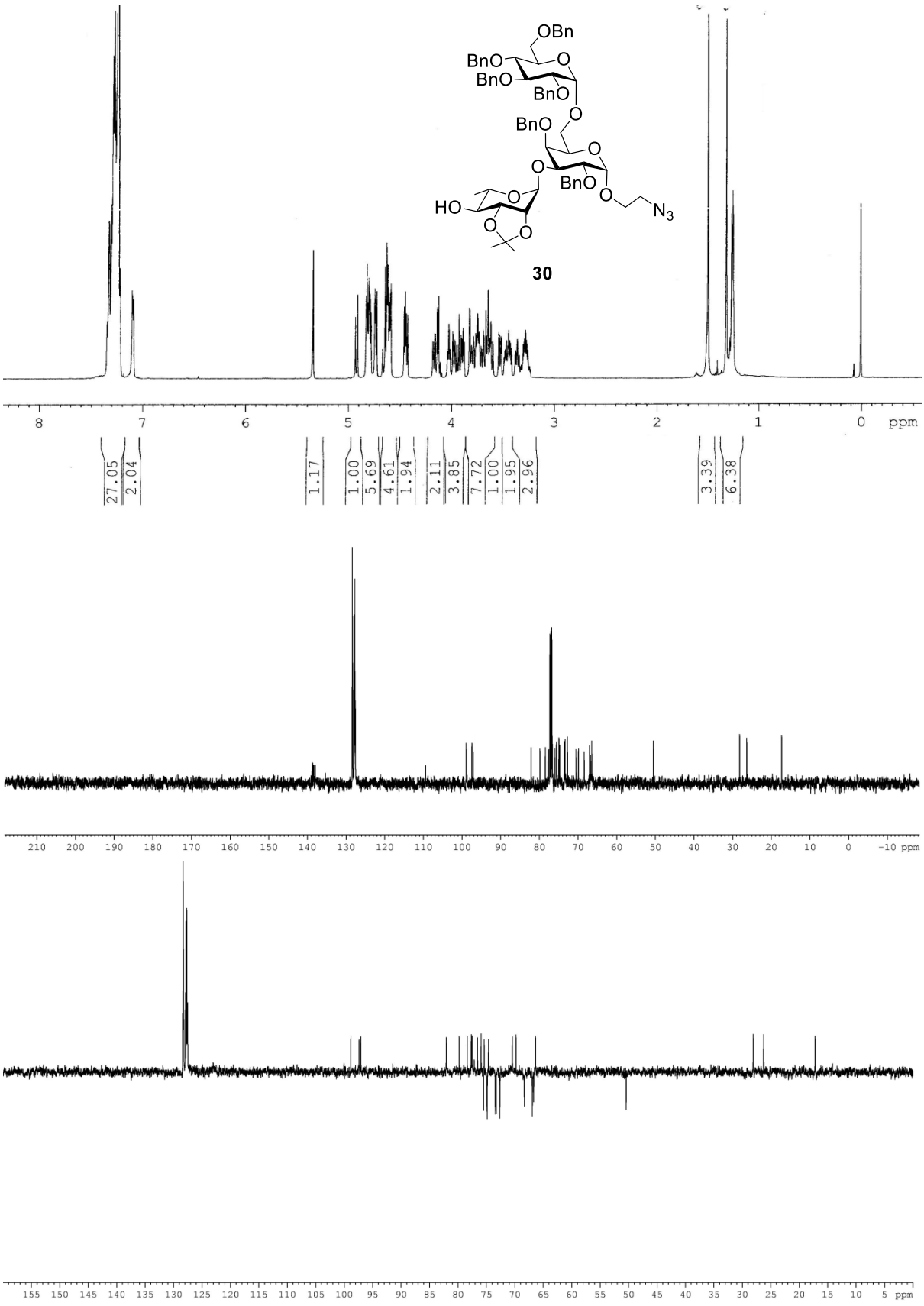

^{1}H, ^{13}C and DEPT-135 NMR spectra of 2-azidoethyl (2,3-*O*-isopropylidene-α-L-rhamnopyranosyl)-(1→3)-[(2,3,4,6-tetra-*O*-benzyl-α-D-glucopyranosyl)-(1→6)]-2,4-di-*O*-benzyl-α-D-galactopyranoside (**30**)($CDCl_3$, 500 MHz).

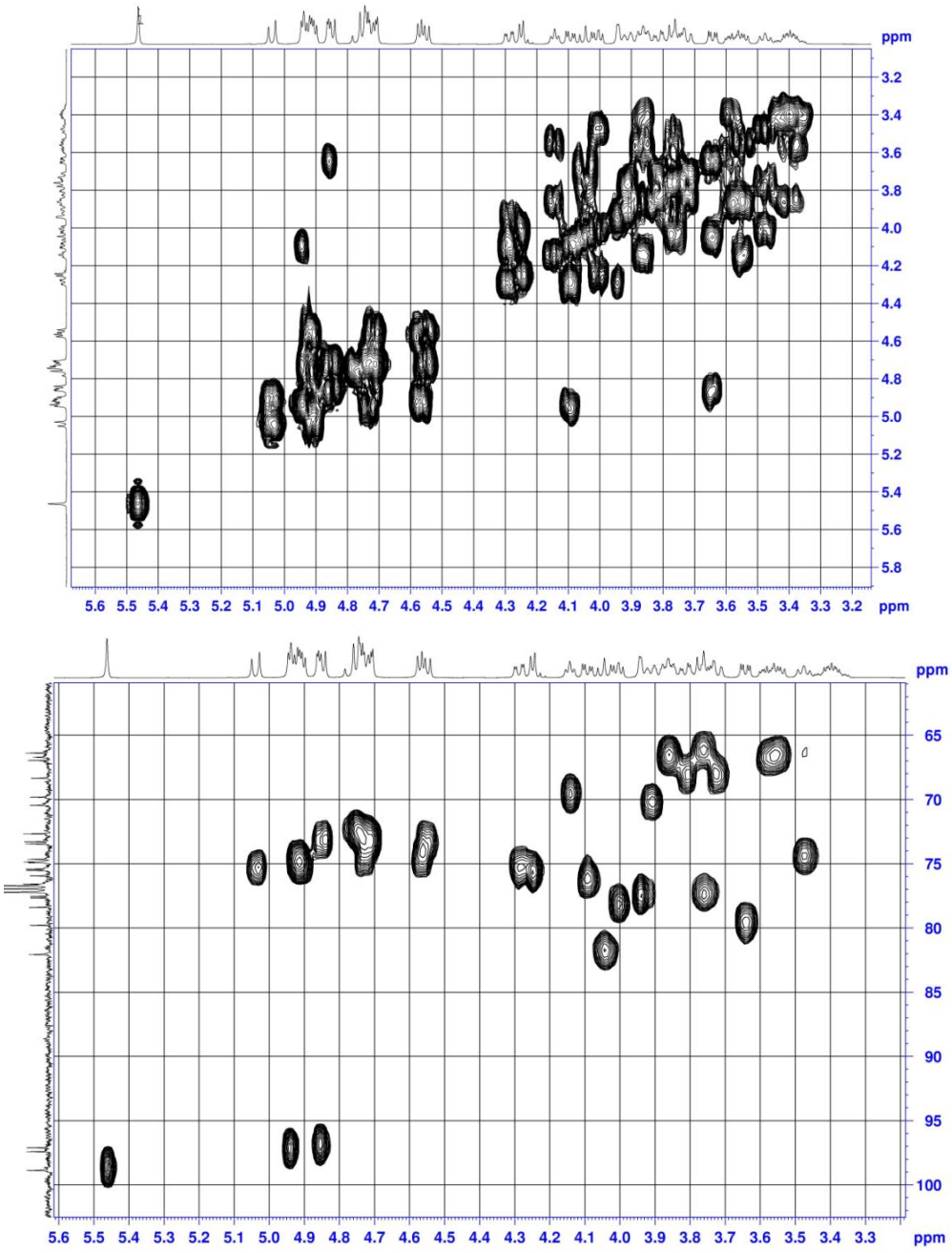

2D COSY and HSQC NMR spectra (selected regions) of 2-azidoethyl (2,3-*O*-isopropylidene-α-L-rhamnopyranosyl)-(1→3)-[(2,3,4,6-tetra-*O*-benzyl-α-D-glucopyranosyl)-(1→6)]-2,4-di-*O*-benzyl-α-D-galactopyranoside (**30**)($CDCl_3$, 500 MHz).

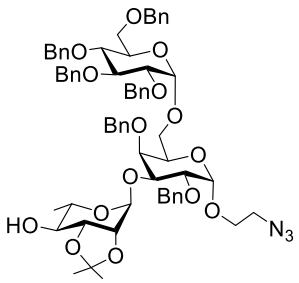

30

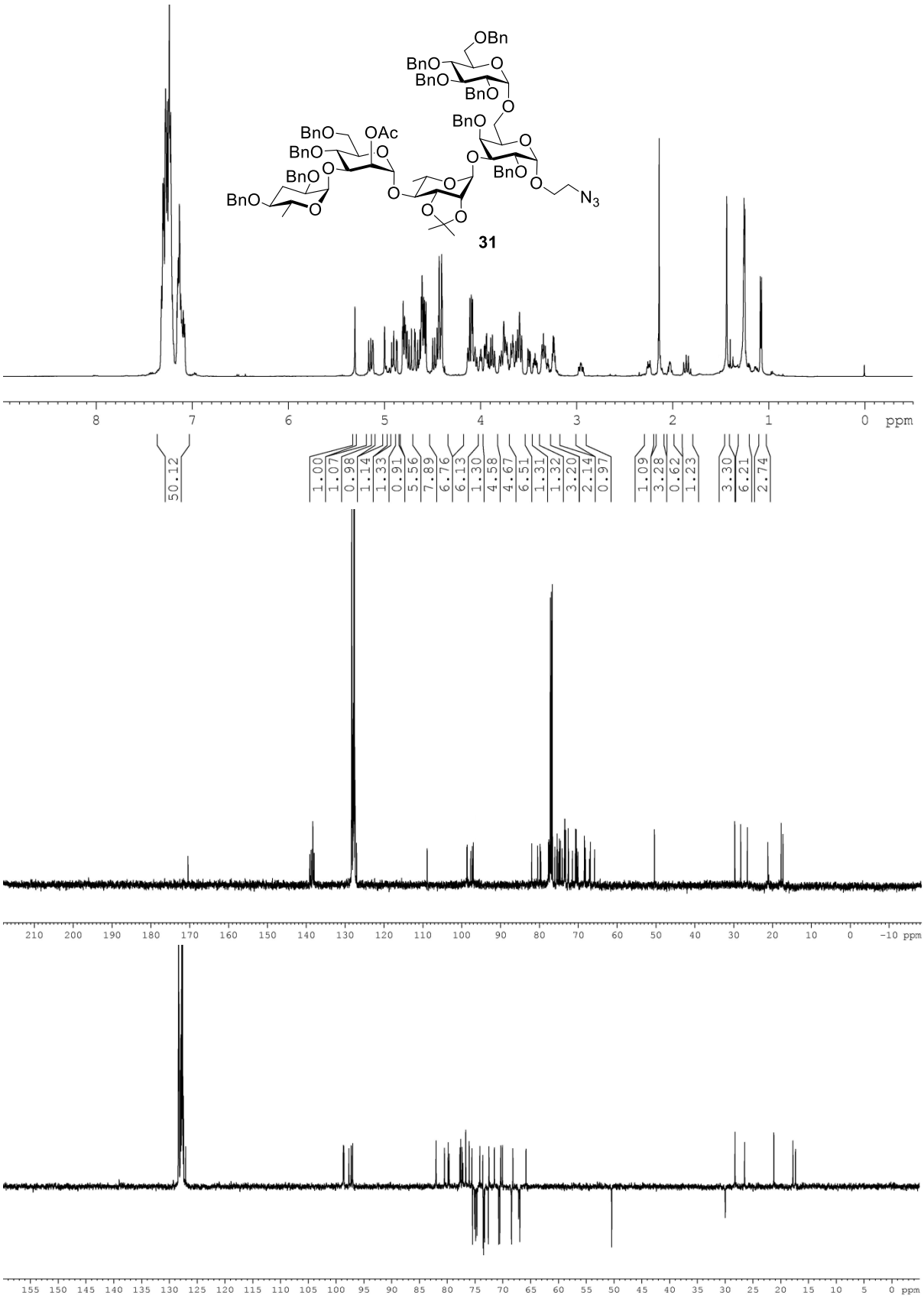

^{1}H, ^{13}C and DEPT-135 NMR spectra of 2-azidoethyl (2,4-di-*O*-benzyl-3,6-dideoxy-α-D-ribo-hexopyranosyl)-(1→3)-(2-*O*-acetyl-4,6-di-*O*-benzyl-α-D-mannopyranosyl)-(1→4)-(2,3-*O*-isopropylidene-α-L-rhamnopyranosyl)-(1→3)-[(2,3,4,6-tetra-*O*-benzyl-α-D-glucopyranosyl)-(1→6)]-2,4-di-*O*-benzyl-α-D-galactopyranoside (**31**) ($CDCl_3$, 500 MHz).

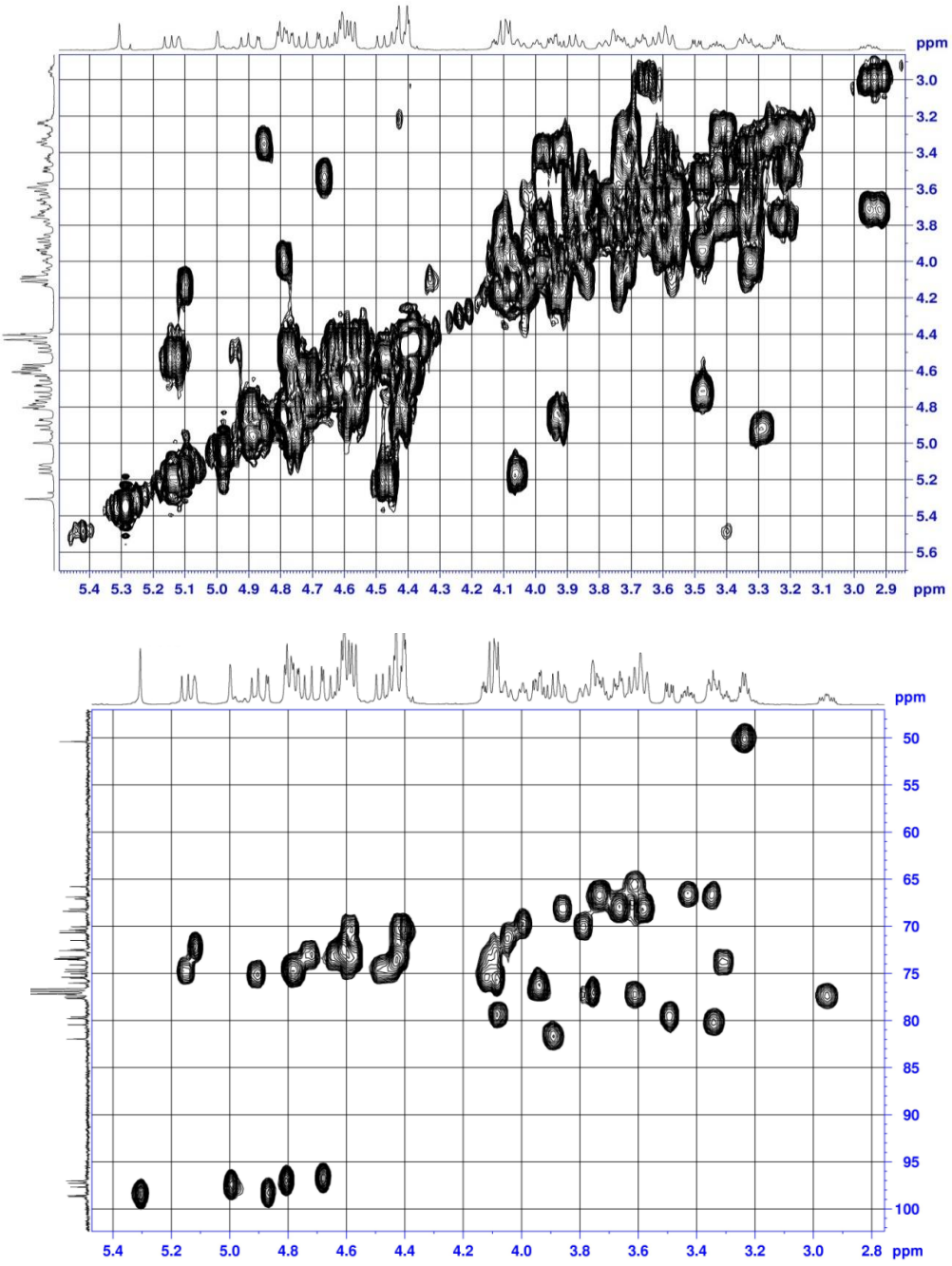

2D COSY and HSQC NMR spectra (selected regions) of 2-azidoethyl (2,4-di-*O*-benzyl-3,6-dideoxy-α-D-ribo-hexopyranosyl)-(1→3)-(2-*O*-acetyl-4,6-di-*O*-benzyl-α-D-mannopyranosyl)-(1→4)-(2,3-*O*-isopropylidene-α-L-rhamnopyranosyl)-(1→3)-[(2,3,4,6-tetra-*O*-benzyl-α-D-glucopyranosyl)-(1→6)]-2,4-di-*O*-benzyl-α-D-galactopyranoside (**31**) ($CDCl_3$, 500 MHz).

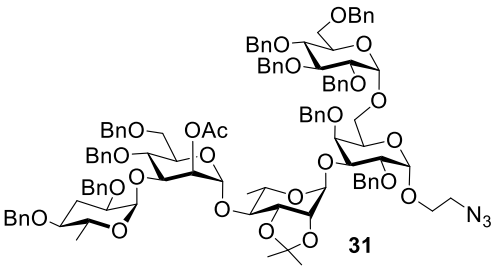

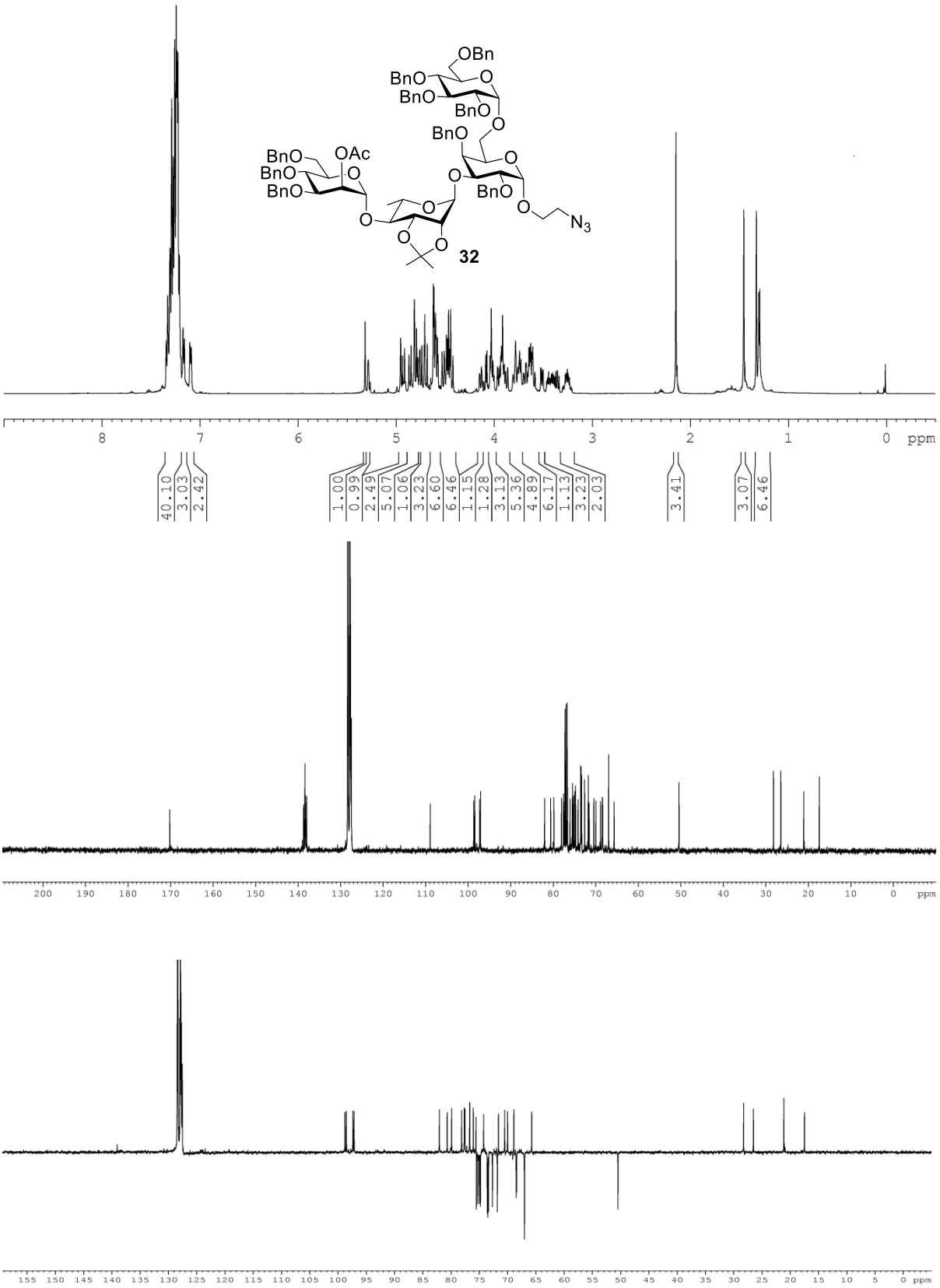

^{1}H, ^{13}C and DEPT-135 NMR spectra of 2-azidoethyl (2-*O*-acetyl-3,4,6-tri-*O*-benzyl-α-D-mannopyranosyl)-(1→4)-(2,3-*O*-isopropylidene-α-L-rhamnopyranosyl)-(1→3)-[(2,3,4,6-tetra-*O*-benzyl-α-D-glucopyranosyl)-(1→6)]-2,4-di-*O*-benzyl-α-D-galactopyranoside (**32**) ($CDCl_3$, 500 MHz).

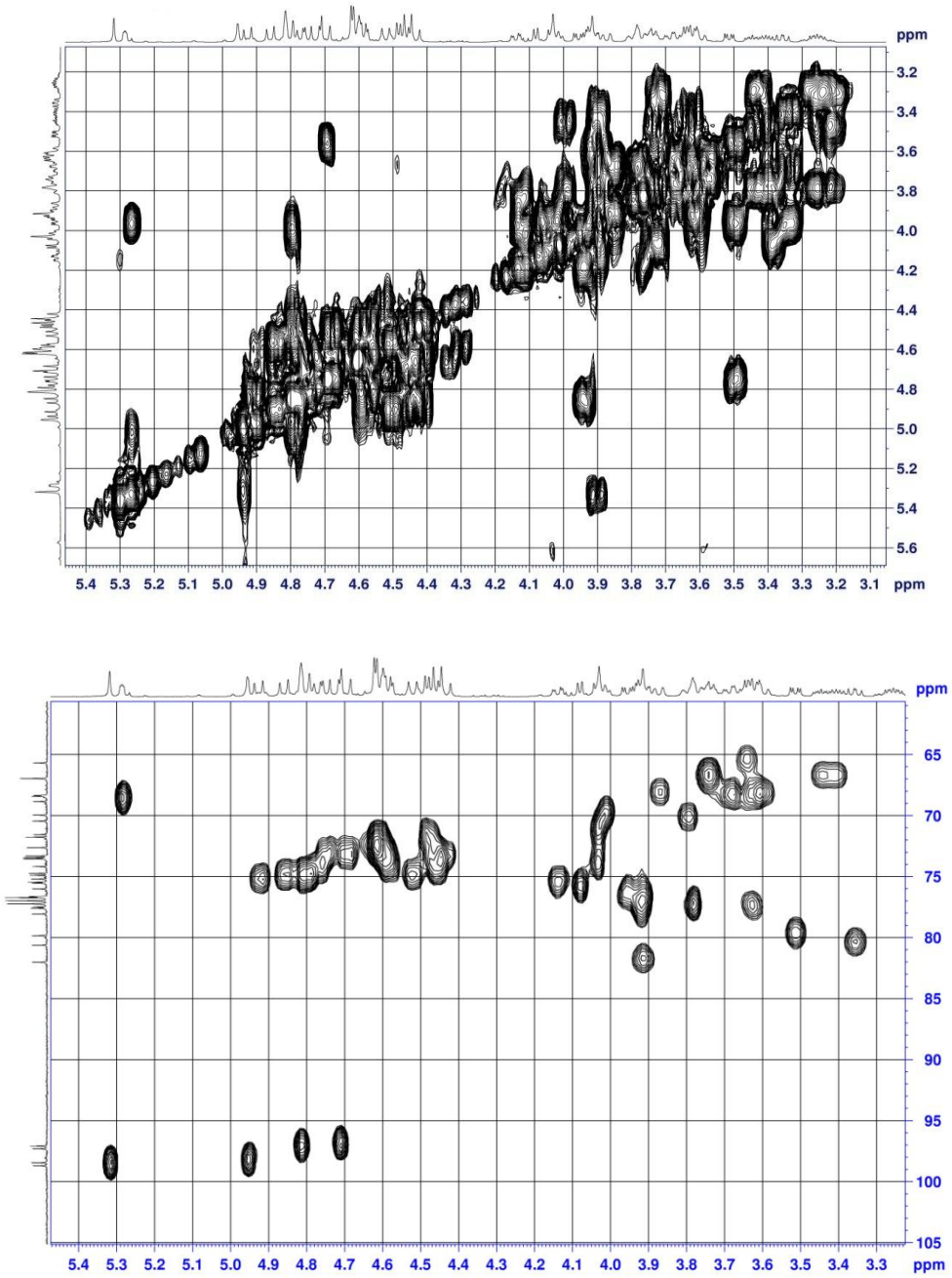

2D COSY and HSQC NMR spectra (selected regions) of 2-azidoethyl (2-*O*-acetyl-3,4,6-tri-*O*-benzyl-α-D-mannopyranosyl)-(1→4)-(2,3-*O*-isopropylidene-α-L-rhamnopyranosyl)-(1→3)-[(2,3,4,6-tetra-*O*-benzyl-α-D-glucopyranosyl)-(1→6)]-2,4-di-*O*-benzyl-α-D-galactopyranoside (**32**) ($CDCl_3$, 500 MHz).